

Reply to the Reviewers' comments

Key:

Review comment.

Response.

“Quotation from revised paper.”

Reply to the Editor

Dear Authors,

Thank you for your detailed responses to the two referees' reports.

Based on my own reading of the manuscript, I find this is an interesting paper that fits the scope of HESS well.

The two reviews are mostly favourable. However, they also make some valid points about providing context/justification, wider implications (in the discussion), subsections, and moving some of the less important figures to supplementary material (e.g. some of the scatterplots).

I would therefore like to invite you to upload a revised manuscript for further review, incorporating the proposed changes and additions, and making any other modifications where you see fit.

I look forward to receiving the revised manuscript.

With best regards,

Louise Slater

We gratefully thank the Editor Louise Slater for her positive comments and suggestions for improvement as well as for handling the review process. We discuss below how we have taken into account the review comments in the revised version.

Reply to Reviewer #1

SUMMARY:

This paper looks at the lagged seasonal correlations between the average river flow in antecedent months and, on one side, peak flow for the High Flow Season (HFS), and on the other hand, average flow for the Low Flow Season (LFS). It also looks at what are the possible physical drivers that could explain these correlations. The study is carried out using a large sample of European rivers. It also shows a real-case application of the findings to flood frequency estimation

GENERAL COMMENTS:

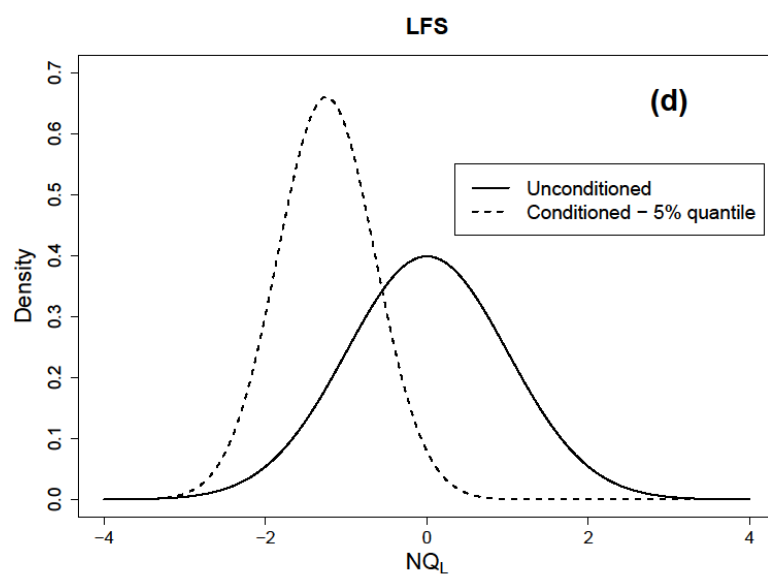
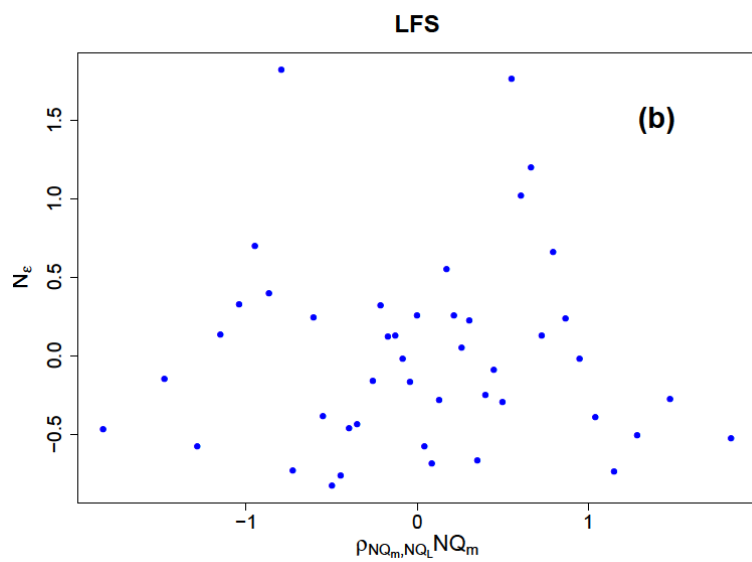
The paper is well-written, clear, interesting and attempts more systematically than previous study to attribute the observed correlations to physical drivers. The methods used are adequate and robust, assumptions are being verified. Overall, it contributes to the advance of science in the field, and my recommendation would therefore be for publication.

We gratefully thank the Reviewer for the very positive evaluation of our work and for recommending publication. We are also thankful for the constructive comments, the corrections and suggestions provided which have certainly helped improve the manuscript. These are discussed below.

However, I have a couple of comments for suggested improvement: 1) My major comment is that, although the whole manuscript looks at both high flows and low flows, and analyses both in detail, the practical example at the end is only for high flows. I think a similar case study for low flows is missing there. If there is a really good reason for only giving an application example for high flows, the motivation for this should be clearly explained.

We thank the Reviewer for this comment. Certainly, the application for LFS is also of great importance and we agree that it would be a useful addition to the paper. Some modifications are required in order to apply the methodology for the case of updating the distribution of average flow in LFS. Following the Reviewer's suggestion, in the revised version, we have presented this application too and discussed it as follows. In order to update the distribution for the average flow in LFS, the already identified average flow in the pre-LFS period serves as the explanatory variable. A linear model is adopted in the Gaussian space in the same manner as for the HFS model. For the case study, we update the low flow distribution upon the hypothetical occurrence of a mean flow in the pre-LFS month equal to its lower 5% sample quantile. The updated distribution in the non-Gaussian space could be modelled by any adequate distribution exhibiting good fit. Among the Gamma, the Weibull and the lognormal distributions, which are typical candidates for average flows, the lognormal distribution was found to exhibit the best fit for the river in question. The above information along with the equations describing the new linear model for the LFS is included in Section 2.3 which is renamed to "Technical experiment: Real-time updating of the frequency distributions for high and low flows". In Section 7, we now include the following plots for the LFS case study alongside the existing plots for the Oise River. In order to maintain the brevity of the manuscript, we have dropped the second HFS application for the Torsebro River. We

have also added discussion on the relevance of the chosen river for preparing for extremes occurring in high and low flow periods (Lines 450-457 of the revised manuscript).



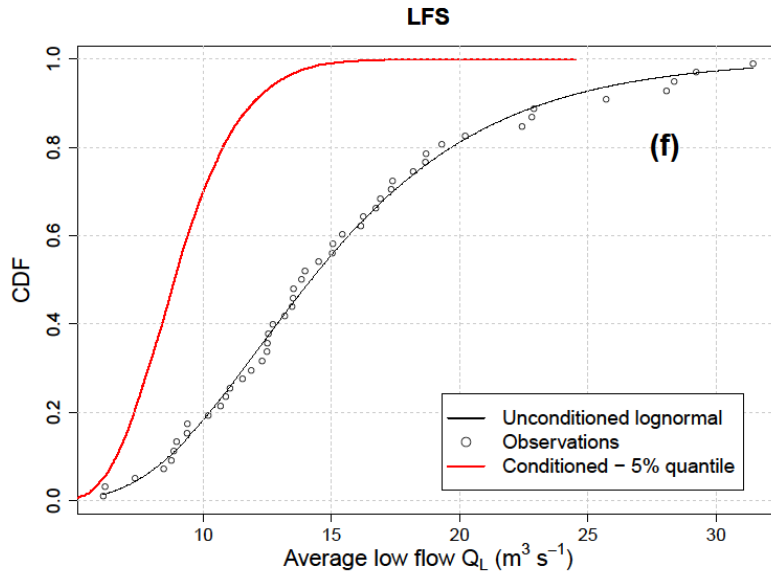


Figure 13. Conditioning the frequency distributions for high and low flows for the Oise River. Plots of the residuals of the linear regression given by Eq. (2) for HFS model (a) and the LFS (b). Probability distribution of the unconditioned normalized peak flows NQ_P (solid line) and the normalized peak flows NQ_P conditioned to the occurrence of the 95% quantile (dotted line) for the HFS (c) and probability distribution of the unconditioned normalized low flows NQ_L (solid line) and the normalized low flows NQ_L conditioned to the occurrence of the 5% quantile (dotted line) for the LFS (d). Gumbel probability plots of the return period vs the unconditioned peak flows Q_P (black line) and the peak flows Q_P modelled by the EV1 distribution and conditioned to the occurrence of the 95% quantile (red line) for the HFS (e) and cumulative distribution function of the unconditioned low flows Q_L (black line) and the low flows Q_L modelled by the lognormal distribution and conditioned to the occurrence of the 5% quantile (red line) for the LFS (f).

Section 2.2 is too long. It would help readability to have a few sub-sections in here. Suggestion of subsections below (could be different, this is just a suggestion): 2.2.1. Correlation analysis 2.2.2. Analysis of physical drivers a) Drivers (catchment descriptors, geological descriptors, climatic descriptors) b) Principal Component Analysis

We thank the Reviewer for this suggestion. We agree and we have adopted the proposed subsections.

MINOR COMMENTS:

Abstract:

line 43: change “in real-world cases” to “in two real-world cases”: otherwise it is misleading and it sounds like you’ve done this to all the 224 catchments

Thanks, we have corrected the wording to “a real-world case”.

1. Introduction:

Line 63-66: Note that the persistence method described by Svensson (2016) that you cite here, has been used operationally in the production of the UK Hydrological Outlook since 2013 (see Prudhomme et al., 2017)

Reference: Christel Prudhomme, Jamie Hannaford, Shaun Harrigan, David Boorman, Jeff Knight, Victoria Bell, Christopher Jackson, Cecilia Svensson, Simon Parry, Nuria Bachiller-Jareno, Helen Davies, Richard Davis, Jonathan Mackay, Andrew McKenzie, Alison Rudd, Katie Smith, John Bloomfield, Rob Ward & Alan Jenkins (2017) Hydrological Outlook UK: an operational streamflow and groundwater level forecasting system C2 at monthly to seasonal time scales, Hydrological Sciences Journal, 62:16, 2753-2768, DOI: 10.1080/02626667.2017.1395032

We thank the Reviewer for bringing to our attention this important application. We have included a short mention to the operational use of the method in Lines 67-69:

“The abovementioned persistence approach has also been used operationally in the production of seasonal streamflow forecasts in the UK since 2013, within the framework of the Hydrological Outlook UK (Prudhomme et al. 2017)”

2. Methodology

Section 2.2: see comment earlier in general comments regarding splitting this section

Thanks, we have addressed this issue as discussed above.

Line 127: change “in terms of catchment, climatic and geological descriptors” to “in terms of catchment, geological and climatic descriptors”, because that is the order in which you list them later in the text.

Thanks, we have changed this.

Line 128-130: add altitude to the list of catchment descriptors (as you present it after percentages of lakes and glaciers).

Thanks, this is added.

Line 139: replace “baseflow index” with “BI”

Thanks, we have changed it.

5. Physical interpretation of correlation

Line 365: typo: replace “20-cathcment” with “20-catchment”

Thank you for the careful review, we have corrected it.

8. Discussion and Conclusions

Line 456: typo: replace “There” with “Their” or “These”

Thanks, we have corrected this too.

Reply to Reviewer #2

Recommendation:

This is a very interesting paper, investigating the drivers of seasonal streamflow correlation for both high and low flows, using a wide range of physical drivers including catchment, geological and climatic descriptors. The paper is very well structured, easy to follow, concise and clear throughout with a well explained methodology and clear contribution to the field. Limitations and assumptions are also discussed well. I would recommend this paper for publication subject to minor revisions based on the comments below.

We are grateful to the Reviewer for providing very positive remarks on the contribution and quality of our work and for recommending publication. We also wish to thank her/him for all the thoughtful suggestions and comments provided which have certainly helped improve the manuscript and highlight its contribution. These are discussed below.

General Comments:

1. It may be apt to mention that this analysis is for Europe, in the title of the paper

Thank you for this suggestion. We have changed the title of the paper to “A large sample analysis of European rivers on seasonal river flow correlation and its physical drivers”.

2. I agree with reviewer 1 that the readability of section 2.2 would improve if it were split into subsections

Thank you for this suggestion. We agree as well and we have adopted Reviewer’s 1 suggestion on that.

3. It is not clear from the methods or from section 7 why you are doing this technical experiment and what you hope to gain from it. There is a brief explanation of this in the abstract, and it would be beneficial to further describe what the purpose of this experiment is within the manuscript.

Thank you for the comment. The technical experiment is meant to highlight the practical applicability of the proposed method, besides its importance for improving the physical understanding of river memory. Providing more reliable flood estimates is a fundamental hydrological task and we want to provide a relevant case study showing how the identified correlation explicitly serves such a purpose. Following the Reviewer’s suggestion, in the revised version, we have elaborated on the purpose of the technical experiment and extended the relevant discussion in the introduction (Lines 91-94) and in the conclusions (Lines 563-573) as well. We have also extended the technical experiment itself (Section 7) to include the low flows distribution updating as well and discussed its practical relevance specifically for the river in question (Lines 450-457):

“The Oise River (55 years of daily flow values) at Sempigny in France has a basin area of 4320 km² and its gauging station at Sempigny is part of the French national real-time monitoring system (<https://www.vigicrues.gouv.fr/>), which is in place to monitor and forecast floods in the main French rivers. The selected river has a high technical relevance since it experiences both types of extremes with large impacts. For instance, a severe drought event in 2005 led to water restrictions impacting agriculture and water

uses in the region (Willsher, 2005), while the river originated an inundation during the 1993 flood events in northern and central France, which was one of the most catastrophic flood-related disasters in Europe in the period 1950-2005 (Barreldo, 2007).

4. Again, I agree with reviewer 1 that I was expecting to a case study / technical experiment for low flows as well, and would like to see this included in the revised manuscript as it would certainly be of interest.

Thank you for the comment. Indeed, this is a very important application too. In the revised version, we have included the relevant case study discussed above.

5. While I find the discussion to be thorough, with comparison to the literature and interesting points made, the conclusions seem to be very rushed and do not do the paper justice. I would recommend including a separate conclusions section and expanding significantly on this, including for example the wider implications of your work, how the findings could be applied and used, what further work could be done from this, etc. The conclusions imply that all of your results agree with the literature that was already out there, when in fact I believe this paper has done more than this. This is also the first time data assimilation is mentioned so there is no context here. It would also be interesting to further mention section 7 as an example of use.

We sincerely thank the Reviewer for the suggestions on how to improve the conclusions in order to better convey the research findings of this work. We have included a separate conclusions section (Section 9, "Conclusions and outlook") and discussed areas of practical applicability as well as directions for further research. We have also mentioned section 7 as an example of use and elaborated on other possible probabilistic models. Additionally, we introduced the data assimilation concept in Section 2.3 (Lines 215-217) as follows:

"In principle, this is a data assimilation approach, since real-time information, i.e. observations of the average river flow, is used in order to update a probabilistic model and inform the forecast of the flow signature of the upcoming season."

6. There are a lot of figures included in this manuscript - is it necessary to include all of these, or could some of them be provided in supplementary material for further interest? Some are barely discussed in the paper, for example 15a,b,c,d.

We thank the Reviewer for this comment. We have added Figures 7 and 11 as supplementary material in the revised version.

– Minor Comments and Clarifications:

Line 33-34: it should be mentioned that the study covers 6 countries in Europe, the abstract implies that the whole of Europe is included

We thank the Reviewer for this remark. We have included this.

Line 78: Remove "in fact"

Thanks, we have removed it.

Lines 87-89: This is repetitive of information stated just above

Thanks, it has been removed.

Line 105: "employed" is used a lot in this paragraph - maybe just use "used"?

Thanks for the suggestion, we have adopted it.

Line 110-111: Why do you not take into account the minor HFS after identifying it? This could be interesting to discuss; but at least should be justified.

We thank the Reviewer for this comment. Actually, we are interested in exploring the river memory for the purpose of predicting high flows and low flows and therefore we are interested in the most extreme seasons. Exploring the memory for the minor HFS may be interesting for reservoir management or water resources management, but in our opinion would not add much for the purpose of analyzing the probability of occurrence of the most relevant flows. Besides, minor high-flow seasons characterized by low or moderate significance were only detected in a few rivers in Austria and Sweden (section 4.1), and therefore, we consider a minor HFS analysis to be more relevant in other regions of the world where bimodal flood regimes are more prominent, as shown by the analysis of Lee et al. (2015). We have add these considerations in Lines 301-305 of the revised manuscript:

“Bi-modality regimes are found with low and moderate significance in rivers located mostly in Austria and Sweden, but we focus here on the major high-flow season, as we are interested in the most extreme events. A minor HFS analysis would be perhaps relevant in other regions of the world where bimodal flood regimes are more prominent, as suggested by the analysis of Lee et al. (2015).”

Line 123: Why do you look for correlation with mean flow in the previous months? This is fine, but the reason should be included.

We use the mean flow in the previous month as a robust indicator of the ‘storage’ in the catchment. The mean flow is more likely to portray the condition of the catchment and its possible change with respect to a higher quantile. The latter correlation is less related to the memory properties of the catchment which are of interest here. We have include the following explanation in the revised version in Lines 130-132.

“We use the mean flow in the previous month as a robust proxy of ‘storage’ in the catchment expected to reflect the state of the catchment, i.e. wetter/drier than usual.”

Line 134: basing -> based

Thanks, we have corrected the wording accordingly.

Line 155: A very brief explanation of flysch and karstic formations would be helpful for those of us with no geological background.

Thanks, we have extend the following phrases giving a brief description of the geology as follows:

“A subset of Austrian catchments is characterized by the dominant presence of flysch, a sequence of sedimentary rocks characterized by low permeability, which is known to generate a very fast flow response.”

“Karstic catchments, characterized by the irregular presence of sinkholes and caves, are also known for having rapid response times and complex behaviour; e.g. initiating fast preferential groundwater flow and intermittent discharge via karstic springs (Ravbar, 2013; Cervi et al., 2017).”

Line 161: Remove "of" ("because of geology...")

Thanks, we have removed it.

Line 165: What type of data is this?

‘Data’ refers to the data described above (mean annual temperature and precipitation), which are gridded. We have added the following clarification in Lines 176-177:

“As climatic descriptors, the mean annual precipitation P (mm year⁻¹) and the mean annual temperature T (°C) are selected. Corresponding gridded data are retrieved...”

Line 166: What is this in km (approx.)?

10 minutes of degree equal approximately 18.55 km at the equator, i.e. the grid size is approx. 344 km², but as the latitude increases towards the poles, the longitude distances decrease. We have included this in parenthesis.

Lines 164-170: You don’t mention here how this relates to snow, which is discussed a lot in the results

Thanks, we have add that low mean temperature regimes are associated with snow (Line 179).

Line 233: Where is this data from? is it observations? please clarify

These are daily streamflow records from gauging stations. These are provided by the institutions mentioned in the authors’ affiliations and are available upon request. We have added the following phrase (Lines 264-265):

“The dataset includes 224 records spanning more than 50 years of daily river flow observations from gauging stations, mostly from non-regulated streams.”

Lines 242-243: Please clarify what Cfb and Dfc climatic types are

Thanks, these acronyms are defined in the legend of Figure 1. We have clarified this and reiterated the explanation in the text as well.

Lines 251: This is indeed interesting, could you expand on which rivers are regulated?

Line 257: Is the regulation really mild; what do you define as mild regulation?

We have information for the presence of such regulation for 16 of the Austrian rivers. We used the term ‘mild’ regulation to describe anthropogenic influences of an intensity that does not majorly alter the flow regimes. These are related to upstream regulation with very low degree of flow attenuation, hydropower operations and flow diversions to and from the basin. Indeed this is a subjective characterization given by the operators of the stations and

unarguably the regulation issue requires more investigation. Unfortunately, the data that we have do not have a time reference (start, duration and end of regulation) nor does the regulation have a common starting period for all the rivers in question. A preliminary examination of these rivers did not reveal any consistent patterns worth discussing. However, because regulation is very common in European rivers, although relevant data are generally lacking (Kuentz et al. 2017) and since the possibility of human influences upstream cannot be excluded even in rivers that are formally denoted as nonregulated, we rely on the assumption of stationarity throughout the manuscript. We have included the above explanation of regulation in Lines 284-293.

“It is relevant to note that 16 of the Austrian rivers are subject to regulation, which may alter the persistence properties of river flows. This relates to generally ‘mild’ forms of regulation, i.e. upstream regulation with very low degree of flow attenuation, hydropower operations and flow diversions to and from the basin. A preliminary examination of these rivers did not reveal any significant change during time of the flow regime. The presence of regulation does not preclude the exploitation of correlation for predicting river flows in probabilistic terms, but may affect the analysis of physical drivers, as it may enhance or reduce persistence in the natural river flow regime. Given that detailed information is generally lacking on the impact of regulation (Kuentz et al. 2017), we assume stationarity of the river flows for all the catchments herein considered and additionally, assume that river management does not significantly affect the identification of the physical drivers.”

Line 287: indexes -> indices

Line 289: available for "a" few countries only.

Thanks, we have corrected the wording accordingly.

Line 204: "it looks that" implies that you are unsure, maybe rephrase this

Lines 349 & 352: again, "looks" implies you are unsure

Thanks for these remarks, we have rephrased.

Line 359: "having" -> "with"

Line 378: summarize -> summarizing

Thanks, we have corrected these accordingly.

Line 378: PCA analysis - analysis is included in this acronym, so reads oddly

Indeed, we have now removed “analysis”.

Line 385: remove "majorly"

Line 391: indexes -> indices

Line 393: remove "also"

Thanks, we have adopted the above suggestions.

Line 407: add "(see sect. 2.3)" after technical experiment

Thanks, we have added this.

Line 435: "within this respect" is odd phrasing, consider rephrasing

Thanks, we have rephrased the wording.

Line 456: there -> their

Line 473: associated to higher -> associated with higher

Thanks, we have corrected the wording accordingly.

Figure 2: Are the boxplots of all the gauging stations? Please clarify in the captions.

Yes they are. We have added this clarification in the caption.

Figure 8: Very nice figure, but you have red dots on top of a green map which should ideally be avoided

Figure 9: Again, a very nice figure, but it's very hard to see the yellow dots

Thank you for pointing this out, indeed this should be avoided. We have changed the color of the dots.

Once again, we would like to thank the Reviewers and the Editor for the very constructive assistance.

References

Lee, D., Ward, P., and Block, P.: Defining high-flow seasons using temporal streamflow patterns from a global model, Hydrol. Earth Syst. Sci., 19, 4689-4705, <https://doi.org/10.5194/hess-19-4689-2015>, 2015.

Kuentz, A., Arheimer, B., Hundecha, Y., and Wagener, T.: Understanding hydrologic variability across Europe through catchment classification, Hydrol. Earth Syst. Sci., 21, 2863-2879, <https://doi.org/10.5194/hess-21-2863-2017>, 2017.

A large sample analysis of European rivers on seasonal river flow correlation and its physical drivers

Theano Iliopoulou^{1*}, Cristina Aguilar², Berit Arheimer³, María Bermúdez⁴, Nejc Bezak⁵, Andrea Ficchi⁶, Demetris Koutsoyiannis¹, Juraj Parajka⁷, María José Polo², Guillaume Thirel⁸ and Alberto Montanari⁹

⁽¹⁾ —Department of Water Resources and Environmental Engineering, School of Civil Engineering, National Technical University of Athens, Zographou, 15780, Greece

⁽²⁾ —Fluvial dynamics and hydrology research group, Andalusian Institute of Earth System Research, University of Cordoba, Cordoba, 14071, Spain

⁽³⁾ Swedish Meteorological and Hydrological Institute, 601 76 Norrköping, Sweden

⁽⁴⁾ —Water and Environmental Engineering Group, Department of Civil Engineering, Universidade da Coruña, 15071 A Coruña, , Spain

⁽⁵⁾ Faculty of Civil and Geodetic Engineering, University of Ljubljana, Jamova 2, SI-1000 Ljubljana, Slovenia

⁽⁶⁾ Department of Geography and Environmental Science, University of Reading, Reading, RG6 6AB, United Kingdom; formerly, IRSTEA, Hydrology Research Group (HYCAR), F-92761, Antony, France

⁽⁷⁾ Vienna University of Technology, Institute of Hydraulic Engineering and Water Resources Management, Karlsplatz 13/222, A-1040 Vienna, Austria

⁽⁸⁾ IRSTEA, Hydrology Research Group (HYCAR), F-92761, Antony, France

⁽⁹⁾ Department DICAM, University of Bologna, Bologna, 40136, Italy

* Correspondence to: Theano Iliopoulou (anyily@central.ntua.gr)

Abstract

The geophysical and hydrological processes governing river flow formation exhibit persistence at several timescales, which may manifest itself with the presence of positive seasonal correlation of streamflow at several different time lags. We investigate here how persistence propagates along subsequent seasons and affects low and high flows. We define the High Flow Season (HFS) and the Low Flow Season (LFS) as the three-month and the one-month periods which usually exhibit the higher and lower river flows, respectively. A dataset of 224 European rivers from six European countries spanning more than 50 years of daily flow data is exploited. We compute the lagged seasonal correlation between selected river flow signatures, in HFS and LFS, and the average river flow in the antecedent months. Signatures are peak and average river flow for HFS and LFS, respectively. We investigate the links between seasonal streamflow correlation and various physiographic catchment characteristics and hydro-climatic properties. We find persistence to be more intense for LFS signatures than HFS. To exploit the seasonal correlation in ~~flood-the~~ frequency estimation of high and low flows, we fit a bivariate Meta-Gaussian probability distribution to the selected flow signatures peak-HFS flow and average ~~pre-HFS-flow~~ in the antecedent months in order to condition the ~~peak-flow~~ distribution of high and low flows in the HFS and LFS, respectively, upon river flow observations in the previous months. The benefit of the suggested methodology is demonstrated by updating the ~~flood~~ frequency distribution of high and low flows one season in advance in a real-world cases. Our findings suggest that there is a traceable physical basis for river memory which in turn can be statistically assimilated into flood-high- and low-flow frequency estimation to reduce uncertainty and improve predictions for technical purposes.

Keywords: ~~flood frequency~~, seasonal streamflow correlation, river memory, persistence, real-time ~~flood-flow~~ forecasting, floods, low flows, meta-Gaussian

1. Introduction

Recent analyses for the Po River and the Danube River highlighted that catchments may exhibit significant correlation between peak river flows and average flows in the previous months (Aguilar et al., 2017). Such correlation is the result of the behaviours of the physical processes involved in the rainfall-runoff transformation that may induce memory in river flows at several different time scales. The presence of long-term persistence in streamflow has been known for a long time since the pioneering works of Hurst (1951) and has been actively studied ever since (e.g. Koutsoyiannis, 2011; Montanari, 2012; O'Connell et al., 2016 and references therein). While a number of seasonal flow forecasting methods have been explored in the literature (e.g. Bierkens and van Beek, 2009; Dijk et al., 2013), attempts to explicitly exploit streamflow persistence in seasonal forecasting through information from past flows have been in general limited. Koutsoyiannis et al. (2008) proposed a stochastic approach to incorporate persistence of past flows into a prediction methodology for monthly average streamflow and found the method to outperform the historical analogue method (see also Dimitriadis et al., 2016 for theory and applications of the latter) and artificial neural network methods in the case of the Nile River. Similarly, Svensson (2016) assumed that the standardized anomaly of the most recent month will not change during future months to derive monthly flow forecasts for 1–3 months lead time and found the predictive skill to be superior to the analogue approach for 93 UK catchments. Notably, the above mentioned persistence approach has also been used operationally in the production of seasonal streamflow forecasts in the UK since 2013, within the framework of known as the Hydrological Outlook UK (Prudhomme et al. 2017). A few other studies have included past flow information in prediction schemes along with teleconnections or other climatic indices (Piechota et al., 2001; Chiew et al., 2003; Wang et al., 2009). Recently, it was shown that streamflow persistence, revealed as seasonal correlation, may also be relevant for prediction of extreme events by allowing one to update the flood frequency distribution based on river flow observations in the pre-flood season and reduce its bias and variability (Aguilar et al., 2017). The above previous studies postulated that

76 seasonal streamflow correlation may be due to the persistence of the catchments storage and/or the weather,
77 but no attempt was made to identify the physical drivers.

78 The present study aims to further inspect seasonal persistence in river flows and its determinants, by
79 referring to a large sample of catchments in 6 European countries (Austria, Sweden, Slovenia, France,
80 Spain and Italy). We focus on persistence properties of both high and low flows by investigating the
81 following research questions: (i) what are the physical conditions, in terms of catchment properties, i.e.
82 geology and climate, which may induce seasonal persistence in river flow? And, (ii) can floods and
83 droughts be predicted, in probabilistic terms, by exploiting the information provided by average flows in
84 the previous months? These questions are relevant for gaining a better comprehension of catchment
85 dynamics and planning mitigation strategies for natural hazards. In fact, we also aim at determining what
86 the physical conditions are, in terms of catchment properties, i.e. geology and climate, which may induce
87 seasonal persistence in river flow. To reach the latter above goals, we identify a set of descriptors for
88 catchment behaviours and climate, and inspect their impact on correlation magnitude and therefore
89 predictability of river flows.

90 A few studies have analysed physical drivers of streamflow persistence on annual and deseasonalized
91 monthly and daily timeseries (Mudelsee, 2007; Hirpa et al., 2010; Gudmundsson et al., 2011; Zhang et al.,
92 2012; Szolgayova et al., 2014; Markonis et al., 2018) but the topic has been less studied on intra-annual
93 scales relevant to seasonal forecasting of floods and droughts.

94 To demonstrate the high practical relevance of the identified seasonal correlations we present a
95 technical experiment for one of the studied rivers (Section 7) in which the frequency distribution of both
96 high and low flows is updated one season in advance by exploiting real-time information on the state of the
97 catchment. Therefore, we herein follow up previous work by further investigating in a larger sample of
98 catchments the predictability of high and low flows in probabilistic terms. Additionally, we inspect the
99 physical drivers of correlation.

100

2. Methodology

The investigation of the persistence properties of river flows focuses separately on both high and low discharges and is articulated in the following steps: (a) identification of the high- and low-flow seasons; (b) correlation assessment between the peak flow in the high flow season (average flow in the low-flow season) and average flows in the previous months; (c) analysis of the physical drivers for streamflow persistence and its predictability through a Principal Component Analysis; (d) real-time updating of the ~~flood~~-frequency distribution of high and low flows for a selected case ~~studies~~-study with significant seasonal correlation by employing a Meta-Gaussian approach. The above steps are described in detail in the following sections.

2.1 Season Identification

Season identification is performed algorithmically to identify the High Flow Season (HFS) and Low Flow Season (LFS) for each river time series. For the estimation of HFS, we employ an automated method recently proposed by Lee et al. (2015), which identifies the high flow season as the three-month period centred around the month with the maximum number of occurrences of Peaks Over Threshold (POT), with the threshold set to the highest 5-% of the daily flows. To evaluate the selection of HFS, a metric constructed as the Percentage of Annual Maximum Flows (PAMF) captured in the HFS is ~~employed~~used. The PAMFs are classified in subjective categories of “poor” (<40-%), “low” (40–60-%), “medium” (60–80 %) and “high” (>80-%) values, denoting the probability that the identified HFS is the dominant high-flow season in the record. If the identified peak month alone contains 80-% or more of annual maxima flows, a uni-modal regime is assumed and the identification procedure is terminated. In all other cases, the method allows for the search of a second peak month and the identification of a minor HFS but we do not further elaborate on this analysis here because ~~we focus on the major HFS~~we are only interested in the most extreme seasons for the purpose of predicting high flows and low flows.

The method proposed by Lee et al. (2015) has several advantages that make it suitable for the purpose of this research. Most importantly, it is capable of handling conditions of bi-modality, which is usually a

major issue for traditional methods like, e.g., directional statistics (Cunderlik et al., 2004). A potential limitation is the assumption of symmetrical extension of HFS around the peak month, along with the uniform selection of its length (3-month period). The degree of subjectivity in the evaluation of the second HFS is another limitation, which is not relevant here as we focus on the main HFS.

LFS is herein identified as the one-month period with the lowest amount of mean monthly flow. An alternative approach of estimating the relative frequencies of annual minima of monthly flow and selecting the month with the highest frequency as LFS is also considered.

2.2 Correlation analysis and physical interpretation through Principal Component Analysis

2.2.1 Correlation analysis

In the case of HFS, a correlation is sought between the maximum daily flow occurring in the HFS period and the mean flow in the previous months. For LFS, correlation is computed between the mean flow in the LFS itself and the mean flow in the previous months. We use the mean flow in the previous month as a robust proxy of ‘storage’ in the catchment expected to reflect the state of the catchment and its possible change, i.e., wetter/drier than usual. Since we are interested in seasonal persistence, we compute the Pearson’s correlation coefficient up to 9-month lag for HFS and 11-month lag for LFS.

2.2.2 Analysis of physical drivers

a. Catchment, geological and climatic descriptors

An extensive investigation is carried out to identify physical drivers of seasonal streamflow correlation, in terms of catchment, ~~geological~~ climatic and ~~geological-climatic~~ descriptors.

As catchment descriptors, we consider the basin area (A), the Baseflow Index (BI), the mean specific runoff (SR), ~~and~~ the percentage of basin area covered by lakes (percentage of lakes, PL) and glaciers (percentage of glaciers, PG) and altitude as candidate explanatory variables for streamflow correlation.

The area A (km^2) is primarily investigated as it is representative of the scale of the catchment, under the assumption that in larger basins the impact of the climatological and geophysical processes affecting river flow becomes more significant and may lead to a magnified seasonal correlation.

Formatted: Subtle Emphasis

Formatted: Normal

Formatted: Subtle Emphasis

Formatted: Subtle Emphasis, Font: Not Bold

Formatted: Subtle Emphasis, Font: Not Bold

Formatted: Subtle Emphasis

Formatted: Indent: First line: 0"

151 BI is considered basing-based on the assumption that high groundwater storage may be a potential
152 driver of correlation. BI is calculated from the daily flow series of the rivers following the hydrograph
153 separation procedure detailed in Gustard et al. (2009). Flow minima are sampled from non-overlapping 5-
154 day blocks of the daily flow series and turning points in the sequence of minima are sought and identified
155 when the 90-% value of a certain minimum is smaller or equal to its adjacent values. Subsequently, linear
156 interpolation is used in between the turning points to obtain the baseflow hydrograph. The ~~baseflow~~
157 ~~index~~BI is obtained as the ratio of the volume of water beneath the baseflow separation curve versus the
158 total volume of water from the observed hydrograph, and an average value is computed over all the
159 observed hydrographs for a given catchment. A low index is indicative of an impermeable catchment with
160 rapid response, whereas a high value suggests high storage capacity and a stable flow regime.

161 SR ($\text{m}^3 \text{s}^{-1} \text{km}^{-2}$) is computed as the mean daily flow of the river standardized by the size of its basin
162 area. It may be an important physical driver as it is an indicator of the catchment's wetness. PL (%) and PG
163 (%) are investigated for the Swedish and Austrian catchments, respectively, as lakes and glaciers are
164 expected to increase catchment storage thus affecting persistence. Lake coverage data are based on
165 cartography and available from the Swedish Water Archive (<https://www.smhi.se/>), while glacier coverage
166 data are estimated from the CORINE land cover database ([https://www.eea.europa.eu/publications/COR0-](https://www.eea.europa.eu/publications/COR0-landcover)
167 [landcover](https://www.eea.europa.eu/publications/COR0-landcover)).

168 The effect of catchment altitude is also inspected using relief maps from the Shuttle Radar
169 Topography Mission (SRTM) data (<http://srtm.csi.cgiar.org/>). The data are available for the whole globe
170 and are sampled at 3 arch-seconds resolution (approximately 90 meters). Topographic information is
171 available for all catchments located at latitude lower than 60 degrees north while a 1 km resolution digital
172 elevation model is available for Austria.

173 As geological descriptors we consider the percentage of catchment area with the presence of flysch
174 (percentage of flysch, PF) and karstic formations (percentage of karst, PK) for Austrian and Slovenian
175 catchments, respectively, for which this type of information is available. A subset of Austrian catchments is

76 characterised by the dominant presence of flysch, a sequence of sedimentary rocks characterized by low
77 permeability, which is known to generate a very fast flow response. Karstic catchments, characterized by
78 the irregular presence of sinkholes and caves, are also known for having rapid response times and complex
179 behaviour; e.g. initiating fast preferential groundwater flow and intermittent discharge via karstic springs
180 (Ravbar, 2013; Cervi et al., 2017). Geological features are expected to be linked to persistence properties
181 also because ~~of~~ geology is the main control for the baseflow index across the European continent (Kuentz
182 et al. 2017). PK (%) and PF (%) are estimated from geological maps of Slovenia and Austria, respectively.

183 As climatic descriptors, the mean annual precipitation P (mm year⁻¹) and the mean annual
184 temperature T (°C) are selected. Corresponding gridded data are retrieved from the Worldclim database
185 (<http://www.worldclim.org/>) at a spatial resolution of 10 minutes of degree (approximately 18.55 km). We
186 note that low mean temperature regimes are also associated with snow, the presence of which is also
187 considered in the interpretation of the results. We also adopt as climatic descriptor the De Martonne index
188 (De Martonne, 1926), IDM, which is given by $IDM = P / (T + 10)$, and enables classification of a region
189 into one of the following 6 climate classes, i.e., arid ($IDM \leq 5$), semi-arid ($5 < IDM \leq 10$), dry sub-humid
190 ($10 < IDM \leq 20$), wet sub-humid ($20 < IDM \leq 30$), humid ($30 < IDM \leq 60$) and very humid ($IDM \geq 60$).
191 Additionally, the Köppen-Geiger climatic classification (Kottek et al., 2006) of the rivers is ~~also~~ assessed.

192 b. Principal Component Analysis

193 To identify what catchment, physiographic and climatic characteristics may explain river memory we
194 attempt to regress the seasonal streamflow correlation against the physical descriptors introduced above.
195 We expect the presence of multi-collinearity among the explaining variables and therefore Principal
196 Component Analysis (PCA; Pearson, 1901; Hotelling, 1933) was applied to construct uncorrelated
197 explanatory variables. In essence, PCA is an orthonormal linear transformation of p data variables into a
198 new coordinate system of $q \leq p$ uncorrelated variables (principal components, PCs) ordered by decreasing
199 degree of variance retained when the original p variables are projected into them (Jolliffe, 2002). Therefore,
200 the first principal axis contains the greatest degree of variance in the data, while the second principal axis is

Formatted: Normal

Formatted: Subtle Emphasis

Formatted: Indent: First line: 0"

the direction which maximizes the variance among all directions orthogonal to the first principal axis and so on. Specifically, let \mathbf{x} be a random vector with mean μ and correlation matrix Σ , then the principal component transformation of \mathbf{x} is obtained as follows:

$$\mathbf{y} = \mathbf{C}^T \mathbf{x}' \quad (1)$$

where \mathbf{y} is the transformed vector whose k th column is the k th principal component ($k=1, 2, \dots, p$), \mathbf{C} is the $p \times p$ matrix of the coefficients or loadings for each principal component and \mathbf{x}' is the standardized \mathbf{x} vector. Standardization is applied in order to avoid the impact of the different variable units on selecting the direction of maximum variance, when forming the PCs. The \mathbf{y} values are the scores of each observation, i.e. the transformed values of each observation of the original p variables in the k th principal component direction.

PCA has useful descriptive properties of the underlying structure of the data. These properties can be efficiently visualized in the biplot (Gabriel, 1971), which is the combined plot of the scores of the data for the first two principal components along with the relative position of the p variables as vectors in the two-dimensional space. Herein, the distance biplot type (Gower and Hand, 1995), which approximates the Euclidean distances between the observations, is used. Variable vectors coordinates are obtained by the coefficients of each variable for the first two principal components. After construction of the PCs, a linear regression model is explored for the case of HFS and LFS lag-1 correlation.

2.3 Technical experiment: Real-time updating of the ~~flood~~-frequency distribution of high and low flows

In order to evaluate the usefulness of the information provided by the one-month-lag seasonal correlation for flow signatures in HFS and LFS, we perform a real-time updating of the ~~flood~~-frequency distribution of high and low flows based on the average river flow~~s~~ in the previous month. A similar analysis for the high flows was carried out by Aguilar et al. (2017) for the Po and Danube Rivers. In principle, ~~This is in principle,~~ a data assimilation approach, since real-time information, i.e. observations of the average river

flow, is used in order to update ~~the existing~~ a probabilistic model and ~~initiate~~ inform a new the forecast for of the flow signature of the upcoming season.

In detail, a bi-variate meta-Gaussian probability distribution (Kelly and Krzysztofowicz, 1997; Montanari and Brath, 2004) is fitted between ~~the observed flow signatures, i.e., observed~~ peak flow in the HFS, ~~Q_p~~ Q_p and ~~average flow in the LFS, Q_l , and~~ the average flow in the pre-flood HFS season and LFS months, Q_m , respectively. The peak HFS flow and the average LFS flow are the dependent variables and ~~is~~ are extracted as the peak river discharge observed in the previously identified HFS and the average river discharge observed in the previously identified LFS, respectively. The average flow in the month preceding the HFS and the LFS is the explanatory variable in both cases. In the following, random variables are denoted by underscore and their outcomes are written in plain form.

The normal quantile transform, NQT (Kelly and Krzysztofowicz, 1997), is used in order to make the marginal probability distribution of dependent and explanatory variables Gaussian. This is achieved as follows: a) the sample quantiles Q are sorted in increasing order e.g. $Q_{m_1}, Q_{m_2} \dots Q_{m_n}$, b) the cumulative frequency, e.g. FQ_{m_i} is computed via a Weibull plotting position, and c) the standard normal quantile, e.g., NQ_{m_i} is obtained as the inverse of the standard normal distribution for each cumulative frequency, ie, e.g., $G^{-1}(FQ_{m_i})$. Therefore, all sample quantiles are discretely mapped into the Gaussian domain. To get the inverse transformation for any normal quantile NQ_{m_i} , we connect the points in the above mapping with linear segments. The extreme segments are extended to allow extrapolation outside the range covered by the observed sample.

In the Gaussian domain, a bivariate Gaussian distribution is fitted between the random explanatory variable NQ_m and the dependent variables ~~NQ_p~~ NQ_p and ~~NQ_l~~ NQ_l by assuming stationarity and ergodicity of the variables. We define the generic random variable NQ_s to represent any dependent flow signature, i.e., in our case, NQ_p and NQ_l in our case. Then, the predicted signature at time t can be written as:

$$NQ_p NQ_{fs}(t) = \rho(NQ_m, NQ_p NQ_{fs}) NQ_m(t) + N\varepsilon(t) \quad (2)$$

Formatted: Font: Italic

Formatted: Not Superscript/ Subscript

Formatted: Underline

Formatted: Not Superscript/ Subscript

Formatted: Underline

Formatted: Underline

Formatted: Underline

Formatted: No underline

Formatted: Font: Italic

Formatted: Font: Italic

Formatted: Font: Italic

Formatted: Font: Italic

Formatted: Font: Italic

where $\rho(\underline{NQ}_m, \underline{NQ}_p, \underline{NQ}_{fs})$ is the Pearson's cross correlation coefficient between \underline{NQ}_m and $\underline{NQ}_p, \underline{NQ}_{fs}$, h is the selected correlation lag with $h = 1$ in the present application, and $N\varepsilon(t)$ is an outcome of the stochastic process $\underline{N\varepsilon}$, which is independent, homoscedastic, stochastically independent of \underline{NQ}_m and normally distributed with zero mean and variance $1 - \rho^2(\underline{NQ}_m, \underline{NQ}_p, \underline{NQ}_{fs})$. Then, the joint bivariate Gaussian probability distribution function is defined by the mean ($\mu(\underline{NQ}_m) = 0$ and $\mu(\underline{NQ}_p, \underline{NQ}_{fs}) = 0$), the standard deviation ($\sigma(\underline{NQ}_m) = 1$ and $\sigma(\underline{NQ}_p, \underline{NQ}_{fs}) = 1$) of the standardized normalized series, and the Pearson's cross correlation coefficient between the normalized series, $\rho(\underline{NQ}_m, \underline{NQ}_p, \underline{NQ}_{fs})$. From the Gaussian bivariate probability properties, it follows that for any observed $\underline{NQ}_m(t - h)$ the probability distribution function of $\underline{NQ}_p, \underline{NQ}_{fs}(t)$ conditioned on \underline{NQ}_m is Gaussian, with parameters given by:

$$\mu(\underline{NQ}_p, \underline{NQ}_{fs}(t)) = \rho(\underline{NQ}_m, \underline{NQ}_p, \underline{NQ}_{fs}) \underline{NQ}_m(t - h) \quad (3)$$

$$\sigma(\underline{NQ}_p, \underline{NQ}_{fs}(t)) = (1 - \rho^2(\underline{NQ}_m, \underline{NQ}_p, \underline{NQ}_{fs}))^{0.5} \quad (4)$$

To derive the probability distribution of $\underline{Q}_{fs}(t)$, i.e. \underline{Q}_p and \underline{Q}_{fs} conditioned to the observed $\underline{Q}_m(t - h)$, we first apply the inverse NQT, i.e., we use linear segments to connect the points of the previous discrete quantile mapping of the original quantiles into the Gaussian domain, and accordingly, obtain $\underline{Q}_{fs}(t)$ for any $\underline{NQ}_{fs}(t)$. to a discrete set of probabilities and Subsequently, we estimated the parameters of an assigned probability distribution for the obtained quantiles in the untransformed domain. This is referred to as the updated probability distribution of the considered flow signature (\underline{NQ}_p and \underline{NQ}_{fs} in our case). We use the Extreme Value Type I distribution for the peak flows and calculate the differences in the magnitude of estimated maxima for a given return period between the unconditioned and the updated distribution. The latter is conditioned by the 95% sample quantile of the observed mean flow in the previous month. To model the low flows we use the lognormal distribution, which was found to exhibit the best fit for the river in question among other typical candidates for average flows, i.e. the Weibull and the Gamma distribution. Respectively, The low flows are conditioned by the lower 5% sample quantile of the observed mean

Formatted: Font: Italic

Formatted: Font: Italic

Formatted: Font: Italic

Formatted: Font: Italic

Formatted: Font: Italic

Formatted: Font: Italic

Formatted: No underline

Formatted: Font: Italic, No underline

Formatted: No underline

Formatted: Font: Italic

Formatted: Font: Italic

Formatted: No underline

Formatted: Font: Italic, No underline

Formatted: No underline

Formatted: Font: Italic, Underline

Formatted: Underline, Subscript

Formatted: No underline

Formatted: Font: Italic, No underline

Formatted: No underline

Formatted: Font: Italic, Underline

Formatted: Font: Italic

Formatted: Font: Italic

Formatted: No underline

Formatted: Font: Italic, No underline

Formatted: No underline

Formatted: No underline

Formatted: Font: Italic, No underline

Formatted: No underline

Formatted: No underline

~~flow in the previous month. To model the low flows we use the lognormal distribution, which was found to exhibit the best fit for the river in question among other typical candidates for average flows, i.e. the Weibull and the Gamma distribution.~~

3. Data and catchments description

The dataset includes 224 records spanning more than 50 years of daily river flow observations from gauging stations~~data~~, mostly from non-regulated streams. A few catchments are impacted by ~~mild~~ regulation. Among the 224 rivers, 108 are located in Austria, 69 in Sweden, 31 in Slovenia, 13 in France, 2 in Spain and one in Italy. Catchment areas vary significantly, the largest being the Po River basin in Italy (70 091 km²) and the smaller being the Hålabäck River basin in Sweden (4.7 km²). The geographical location of the river gauge stations as well as their climatic classification ~~is~~are shown in Fig. 1. Most of the examined rivers belong to either a warm temperate (C) or a boreal/snow climate (D) with a subset impacted by polar climatic conditions (E), according to the updated World Map of the Köppen-Geiger climate classification (Fig. 1) based on gridded temperature and precipitation data for the period 1951-2000 (Kottek et al., 2006). More specifically, the majority of French, Slovenian and approximately one third of the Swedish basins belong to the warm temperate Cfb category characterized by precipitation distributed throughout the year (fully humid) and warm summers. The rest of the Swedish catchments are impacted by a Dfc climatic type, i.e. a snow climate, fully humid with cool summers. The Austrian catchments belonging to the region impacted by the European Alps have the most complicated regime due to their topographic variability. At the lowest altitudes, Cfb is the prevailing regime, but as proximity to the Alps increases, a Dfc regime dominates and progressively, in the highest altitude basins, the climate becomes a polar tundra type (Et), characterized primarily by the very low temperatures present. The characteristics of all the climatic regimes of the studied rivers are given in the legend of Fig. 1. A summary of the river basins under study in terms of the selected descriptors is also provided in Table 1, showing that the investigated rivers cover a wide range of catchment area sizes, flow regimes and climatic conditions.

It is ~~interesting-relevant~~ to note that ~~some-16~~ of the ~~above-Austrian~~ rivers are subject to regulation, which may alter the persistence properties of river flows. ~~This relates to generally ‘mild’ forms of regulation, i.e. upstream regulation with very low degree of flow attenuation, hydropower operations and flow diversions to and from the basin. A preliminary examination of these rivers did not reveal any significant change during time of the flow regime. The presence of regulation does not preclude the exploitation of correlation for predicting river flows in probabilistic terms, but may affect the analysis of physical drivers, as it may enhance or reduce persistence in the natural river flow regime. Given that detailed information is generally lacking on the impact of regulation (Kuentz et al. 2017), we assume stationarity of the river flows for all the catchments herein considered and additionally, assume that river management does not significantly affect the identification of the physical drivers.~~ ~~On the one hand, under the assumption that river flow management does not change in time, the presence of regulation does not preclude the exploitation of correlation for predicting river flows in probabilistic terms. On the other hand, regulation may affect the analysis of physical drivers, as it may enhance or reduce persistence in the natural river flow regime~~

~~Given that the results that we herein present are derived from a large sample of catchments, we assume that they are not significantly affected by the above-mentioned types of mild regulation that takes place in a few of them.~~

4. River memory analysis for the considered case studies

4.1 Season Identification

Approximately half of the 224 rivers are characterized by at least one high-flow season with medium or higher significance ($\text{PAMF(HFS)} \geq 60\%$). Among them, very strong unimodal regimes ($\text{PAMF(HFS)} \geq 80\%$) are observed in 63 rivers, the majority of which are located in Sweden. For 25% of the rivers, a high-flow season of low significance is found (PAMF(HFS) between 40–60%), while for the remaining 25% the high-flow distribution looks uniform along the year. Bi-modality regimes are found with low and moderate significance in rivers located mostly in Austria and Sweden, but we focus here on the major high-

flow season, ~~for which we inspect higher seasonal correlation against previous average flows we are~~
~~interested in the most extreme events. A minor HFS analysis would be perhaps relevant in other regions of~~
~~the world where bimodal flood regimes are more prominent, as suggested by the analysis of Lee et al.~~
~~(2015).~~

Regarding the LFS identification, the two considered approaches (see Section 2.1) agree for 139 out
of 224 stations but the first method, i.e. the one-month period with the lowest amount of mean monthly
flow is selected as being more relevant to the purpose of computing mean flow correlations.

4.2 Seasonal correlation

LFS correlation is markedly higher than the corresponding HFS correlation for lags 1–5 and its median
remains higher than 0 for more lags (see Fig. 2). For the case of HFS correlation, we focus only on the most
significant first lag, for which 73 rivers are found to have correlation significantly higher than 0 at 5-%
significance level. In Fig. 3, the autocorrelation of the whole monthly series is compared to the LFS
correlation for lag of 1 and 2 months, in order to prove that the seasonal correlation for LFS is significantly
higher than its counterpart computed by considering the whole year. The latter is also confirmed by the
Kolmogorov-Smirnov test for both LFS lags (corresponding p-values, $p_{lag1} < 2.2 \times 10^{-6}$ and $p_{lag2} < 2.2 \times 10^{-6}$
for the null hypothesis that the LFS correlation coefficients are not higher than the corresponding values for
the monthly series autocorrelation; Conover, 1971).

Figure 4 shows the spatial pattern of HFS and LFS streamflow correlations. It is interesting to notice
the emergence of spatial clustering in the correlation magnitude, which implies its dependence on different
spatially varying physical mechanisms. For example, for HFS, a geographical pattern emerges within
France, since the highest correlation coefficients are located in the northern part of the country, which is
characterized by oceanic climate and higher baseflow indexes.

5. Physical interpretation of correlation

To attribute the detected correlations to physical drivers, we define 6 groups of potential drivers of seasonal correlation magnitude, which are: basin size, flow ~~indexes~~indices, presence of lakes and glaciers, catchment elevation, catchment geology, and hydro-climatic forcing. For some of the descriptors the information is available for a few countries only.

In what follows, we will use the term “positive (negative) impact on correlation” to imply that an increasing value of the considered descriptor is associated to increasing (decreasing) correlation. For each descriptor, we also report between parentheses the Spearman’s rank correlation coefficient r_s (Spearman, 1904) between its value and the considered (LFS or HFS) correlation, and the p-value of the null hypothesis $r_s = 0$. Spearman’s coefficient is adopted in view of its robustness to the presence of outliers and its capability of capturing monotonic relationships of non-linear type.

5.1 Catchment area – Descriptor A

Figure 5 shows that there is only a weak positive impact of the catchment area (log-transformed) on correlation for HFS ($r_s = 0.17$, $p = 0.01$) but a more significant positive one for LFS ($r_s = 0.27$, $p = 5.5 \times 10^{-5}$). ~~We expected a more pronounced positive impact of the catchment area.~~ The presence of relevant scatter in the plots also indicates that it is not a key determinant of correlation.

5.2 Flow ~~indexes~~indices – Descriptors BI and SR

The effect of the BI and SR is shown in Fig. 6. BI (Fig. 6a) appears to be a marked positive driver for LFS ($r_s = 0.6$, $p = 1.8 \times 10^{-23}$) while its effect for HFS is less clear, being weakly positive ($r_s = 0.21$, $p = 0.001$). ~~As for~~ SR (Fig. 6b), it ~~looks~~appears that both LFS and HFS streamflow correlations drop for increasing wetness ($r_s = -0.4$, $p = 4 \times 10^{-10}$ and $r_s = -0.28$, $p = 2.8 \times 10^{-5}$ respectively).

5.3 Presence of lakes and glaciers – Descriptors PL and PG

Detailed information on the presence of lakes is available for the 69 Swedish catchments while areal extension of glaciers is known for the 108 Austrian catchments. Figure ~~7-S1 in the Supplement~~ shows ~~their~~

370 ~~impact that~~ The ~~the~~ impact of lake area (Fig. ~~7A~~8~~S1a~~) on correlation for LFS and HFS is not significant but
371 positive ($r_s = 0.10$, $p = 0.399$ and $r_s = 0.12$, $p = 0.347$). The results for glaciers show a positive impact for
372 LFS ($r_s = 0.28$, $p = 0.081$) but negative for HFS ($r_s = -0.34$, $p = 0.032$). For a meaningful interpretation,
373 these results should be considered in conjunction with the seasonality of flows for the Austrian catchments.
374 Low flows for the glacier-dominated catchments are typically occurring in winter months, when glaciers
375 are not contributing to the flow (Parajka et al., 2009). Thus the observed result for LFS is more likely
376 portraying the impact of low temperature (low evapotranspiration) and snow accumulation, the latter
377 generally being a slowly varying process. For HFS, which is typically occurring in the summer months for
378 the considered catchments, flows are mainly determined by snowmelt which is associated to large
379 variability and reduced persistence (Fig. ~~7B~~8~~S1b~~).

380 5.4 Catchment elevation

381 The areal coverage of the SRTM data is limited to 60 degrees north and 54 degrees south and therefore,
382 data for the northern part of the Swedish catchments are not available. The rest of the rivers are divided in
383 three regions based on proximity: Region I including the central and eastern part of the Alps and
384 encompassing Austrian, Slovenian and Italian catchments; Region II showing the western part of the Alps
385 and encompassing French and Spanish territory; and Region III including the southern part of Sweden.
386 Figure 8 shows elevation maps along with the location of gauge stations and magnitude of correlations.
387 Elevation seems to enhance LFS correlation which is more evident in the mountainous Region I (Fig. ~~8~~7).
388 For HFS correlation there is not a prevailing pattern.

389 In the case of Austrian catchments, a 1 km resolution digital model is also used to extract information
390 on elevation. Figure ~~9~~8 confirms that there is a positive correlation pattern emerging with elevation for
391 LFS. Based on local climatological information, it can be concluded that the spatial pattern for LFS
392 correlation is reflective of the timing and strength of seasonality of the low flows in Austria, where dry
393 months occur in lowlands during the summer due to increased evapotranspiration and in the mountains
394 during winter (mostly February) due to snow accumulation which is characterised by stronger seasonality

395 compared to the lowlands flow regime (Parajka et al., 2016; see Fig. 1). Concerning HFS in the same
 396 region, high flows are significantly impacted by the seasonality of extreme precipitation (Parajka et al.,
 397 2010), which is highly variable, with the exception of the rivers where high flows are generated by
 398 snowmelt. Therefore, a spatially consistent pattern does not clearly emerge.

399

400 5.5 Catchment geology – Descriptors PK and PF

401 Two different geological behaviours are identified which may impact river correlation. We first focus on 21
 402 Slovenian catchments (out of 31) where more than 50-% of the basin area is characterised by the presence
 403 of karstic aquifers (percentage of karstic areas $PK \geq 50\%$). Figure ~~40-9~~ shows boxplots of the estimated
 404 lag-1 correlation coefficient for both HFS and LFS against rivers where $PK < 50\%$. It is clear that there is a
 405 significant decrease in correlation where karstic areas dominate for both for HFS and LFS.

406 In a second analysis, we focus on Austrian catchments and investigate the relationship between
 407 correlation and percentage of Flysch coverage, PF. Figure ~~44-S2 in the Supplement~~ shows that there is not a
 408 prevailing pattern in either case ($r_s = 0.13$, $p = 0.6$ for LFS and $r_s = -0.19$, $p = 0.446$ for HFS).

409 5.6 Atmospheric forcing – Descriptors P and T

410 Figure ~~42-10~~ shows the lag-1 HFS and LFS correlations against estimates of the annual precipitation P and
 411 annual mean temperature T as well as the De Martonne index IDM. LFS correlation ~~looks-appears to be~~
 412 more sensitive than HFS to the above climatic indices, showing a decrease with increasing temperature and
 413 also a decrease with increasing precipitation ($r_s = -0.44$, $p = 3.1 \times 10^{-12}$ for P and $r_s = -0.57$, $p = 1.8 \times 10^{-20}$
 414 for T). HFS correlation ~~looks—is~~ scarcely sensitive to these variables ($r_s =$
 415 -0.17 , $p = 0.011$ for P and $r_s = 0.08$, $p = 0.208$ for T). The IDM (Fig. ~~42-10~~ c) shows a mild decrease of
 416 both LFS ($r_s = -0.06$, $p = 0.368$) and HFS correlation with increasing IDM ($r_s = -0.17$, $p = 0.01$), while for
 417 the latter there seems to be a clearer trend (lower correlation with higher IDM) in very humid areas (dark
 418 blue points in Fig. ~~42e10c~~).

419

420 **5.7 Physical drivers of high correlation**

421 To gain further insights into the results we select the 20 catchments ~~having-with~~ the highest streamflow
422 seasonal correlation coefficients for both HFS and LFS periods in order to investigate their physical
423 characteristics in relation to the remaining set of rivers. Table 2 summarizes statistics for selected
424 descriptors in order to identify dominant behaviours. We also compare the number of rivers with distinctive
425 features, i.e. lakes N_L (number of rivers with lakes), glaciers N_G (number of river with glaciers), flysch N_F
426 (number of rivers with flysch formations) and karst N_K (number of rivers with karstic areas) for the highest
427 correlation group with those obtained from 1000 randomly sampled 20-catchment groups from the whole
428 set of considered catchments to assess whether higher correlation implies distinctive features.

429 By focusing on HFS, one can notice that the catchments with higher seasonal correlation are
430 characterised by larger catchment area, higher baseflow index and temperature with respect to the
431 remaining catchments, and lower specific runoff, precipitation and wetness. Presence of lake, glaciers,
432 karstic and Flysch areas do not appear significantly effective at a 5-% significance level. More robust
433 considerations can be drawn for the LFS: higher seasonal correlation is found for larger catchments with
434 higher baseflow index and lower specific runoff, precipitation and wetness. Decreasing temperature is
435 strongly associated with higher correlation for the LFS. The presence of lakes plays a significant role both
436 for lag-1 and lag-2 correlations with the latter being also significantly influenced by presence of glaciers.

437 **6. Principal component analysis of the predictors and linear regression**

438 We attempt to fit a linear regression model to relate correlation to physical drivers, in order to support
439 correlation estimation for ungauged catchments. To avoid the impact of multicollinearity in the regression
440 while additionally ~~summarize-summarizing~~ river information, we apply a-PCA ~~analysis~~ (see Section 2.2).
441 Although correlation effects are efficiently dealt with via the PCA, we avoid including highly correlated
442 variables in the analysis. For example, the De Martonne Index, Precipitation and SR are mutually highly

443 correlated (all Pearson's cross-correlations are higher than 0.6) and therefore we only consider the SR in
444 the PCA because it shows a more robust linear relationship with correlation magnitude. We select A, BI,
445 SR and T as the variables to be considered in the PCA. A log transformation is applied on the basin area to
446 reduce impact of outliers. Table 3 shows the coefficients estimated for each component (the loadings) and
447 the explained variance. The first principal component is primarily a measure of BI; the second principal
448 component ~~majorly~~ mostly accounts for T and the third principal component accounts for A. There is an
449 evident geographical pattern emerging by the visualization of countries in the biplot (Fig. ~~4311~~). Slovenian
450 rivers cluster towards the direction of increasing SR and T , whereas Swedish rivers towards the opposite
451 direction of increasing BI and decreasing T . Austrian rivers, which are the majority, are the most diverse.
452 The first two components together explain the 70-% of the total variability in the data.

453 Naturally, the statistical behaviour of the ~~indexes~~ indices reflects the known local controls for certain
454 rivers. For example, the observed lowest BI in Slovenia is consistent with the presence of karstic
455 formations for the majority of the Slovenian rivers, as ~~also~~ is the higher BI in Sweden and Austria, which is
456 related to the presence of lakes and glaciers in both countries.

457 In the case of HFS, all the examined linear models (combinations of $\ln A$, SR, BI, P , T , IDM
458 predictors) failed in explaining the streamflow correlation magnitude. On the contrary, the linear regression
459 model performs fairly well in explaining the correlation for LFS, with an adjusted R^2 value of 0.58 and an
460 F-test returning a p-value $< 2.2 \times 10^{-16}$. The coefficients for the first three PCs are found significantly
461 different from zero at a 0.1-% significance level and are included in the regression (see Table 4). The
462 highest coefficient is obtained for the first PC, which mostly accounts for BI importance. Diagnostic plots
463 from linear regression for LFS are shown in Fig. ~~4412~~. There is no clear violation of the homoscedasticity
464 assumption in linear regression, apart from the presence of a limited number of outliers. There is a certain
465 departure from normality in the lower tail of the residuals, which relates to the fact that the model performs
466 better in the area of higher seasonal streamflow correlations and overestimates the lower correlations.

467

7. Real-time updating of the ~~flood~~-frequency distribution of high and low flows for ~~selected~~ the Oise River

We apply the technical experiment (see section 2.3) for high and low flows to ~~two the Oise River in~~
~~France~~ with significant lag-1 streamflow correlation for HFS and assess the difference in the estimated
flood and low-flow magnitudes. We update the probability distribution of high and low flows after the
occurrence of the upper 95% and lower 5% sample quantile of the observed mean flow in the previous
month, respectively.

The ~~first river is the~~ Oise River (55 years of daily flow values) at Sempigny in France ~~with has a basin area~~
~~of 4320 km² and its gauging station at Sempigny is part of the French national real-time monitoring system~~
~~(<https://www.vigicrues.gouv.fr/>), which is in place to monitor and forecast floods in the main French rivers.~~
~~The selected river has a high technical relevance since it experiences both types of extremes with large~~
~~impacts. For instance, a severe drought event in 2005 led to water restrictions impacting agriculture and~~
~~water uses in the region (Willsher, 2005), while the river originated an inundation during the 1993 flood~~
~~events in northern and central France, which was one of the most catastrophic flood-related disasters in~~
~~Europe in the period 1950-2005 (Barreldo, 2007). It is characterized by HFS correlation $\rho = 0.54$, which is~~
~~the 3rd largest lag-1 correlation for the HFS in our dataset and LFS correlation $\rho = 0.80$, which stands for~~
~~the 70-% quantile of the sample lag-1 correlation for LFS. The second river is the Torsebro River at Helge~~
~~in Sweden (53 years of daily flow values). Its lag-1 correlation coefficient for the HFS equals 0.46 which~~
~~ranks 9th among the rivers. The Torsebro River has a catchment area of 3665 km² with lake coverage of 5.4~~
~~%, while the Oise River catchment is slightly larger (4320 km²).~~

A visual inspection of the residuals plots ~~for both rivers~~ is also performed (Fig. ~~45-13a~~, b) in order to
evaluate the assumption of homoscedasticity of the residuals of the regression models given by Eq. (2). The
residuals do not show any apparent trend and therefore the Gaussian linear model is accepted. Figure ~~45-13~~
(c, d) shows the conditioned and unconditioned probability distributions of peak and low flows in the

Formatted: Font: Italic

Gaussian domain. As expected from Eq. (3) and (4), the variance of the updated (conditioned) distributions decreases while the mean value increases.

After application of the inverse NQT the conditioned peak flows are modelled through the EV1 distribution and compared to the unconditioned (observed) peak flows. The corresponding Gumbel probability plots for conditioned and unconditioned distributions ~~are-is~~ shown in Fig. 153 (e, f) ~~for the two rivers~~. For the return period of 200 years, the updated distribution shows a 6-% increase in the flood magnitude for the Oise River ($307.7 \text{ m}^3 \text{ s}^{-1}$ to $326.44 \text{ m}^3 \text{ s}^{-1}$) ~~and a 10-% increase for the Torsebro River ($298.07 \text{ m}^3 \text{ s}^{-1}$ to $329.22 \text{ m}^3 \text{ s}^{-1}$)~~. Likewise, the conditioned low flows are modelled through the lognormal distribution. The two cumulative distribution functions are compared in Fig. 13f showing a major departure in the estimated quantiles for the updated distribution; the occurrence of the predefined 5-% quantile flow in the pre-LFS month induces a decrease of the exceedance probability of an average LFS flow of $15 \text{ m}^3 \text{ s}^{-1}$ from a prior 43% (according to the unconditioned model) to 1%.

8. Discussion and Conclusions

The methodology presented herein aims to progress our physical understanding of seasonal river flow persistence for the sake of exploiting the related information to improve probabilistic prediction of high and low flows. The correlation of average flow in the previous months with LFS flow and HFS peak flow was found to be relevant, with the former prevailing on the latter. This result was expected since the LFS correlation refers to average flow while the HFS correlation is related to rapidly occurring events. We also aim to investigate physical drivers for correlation. Therefore, a thorough investigation of the geophysical and climatological features of the considered catchments was carried out.

We found that increasing basin area and baseflow index are associated with increasing seasonal streamflow correlation. ~~Within To~~ this respect, Mudelsee (2007), Hirpa et al. (2010) and Szolgayova et al. (2014a) also found positive dependencies of long-term persistence on basin area, Markonis et al. (2018) found a positive impact too but for larger spatial scales ($> 2 \times 10^4 \text{ km}^2$), while Gudmunsson et al. (2011) found basin area to have negligible to no impact to the low-frequency components of runoff. Our results

517 additionally point out that catchment storage induces mild positive correlation, not only for low discharges
518 which are directly governed by base flow, but also for high flows.

519 Previous studies also pointed out that correlation increases for groundwater-dominated regimes
520 (Yossef et al., 2013; Dijk et al., 2013; Svensson, 2016) and slower catchment response times (Bierkens and
521 van Beek, 2009), which concurs with the impact of baseflow index found herein as well as with the
522 observed impact of fast responding karst areas. The latter findings are also in agreement with our
523 conclusion that correlation decreases for increasing rapidity of river flow formation, which for instance
524 occurs in the presence of karstic areas and wet soils, which explains why persistence decreases with high
525 specific runoff; as also confirmed by other studies (Gudmundsson et al., 2011; Szolgayova et al., 2014).

526 Other contributions also reported higher streamflow persistence in drier conditions, either relating to
527 lower specific runoff or mean areal precipitation estimates (Szolgayova et al., 2014; Markonis et al., 2018).
528 It was postulated that this is due to wet catchments showing increased short-term variability compared to
529 drier catchments (Szolgayova et al., 2014) and having a faster response to rainfall due to saturated soil. A
530 similar conclusion has been reached by other previous studies reporting that low humidity catchments are
531 more sensitive to inter-annual rainfall variability (Harman et al., 2011), therefore leading to enhanced
532 persistence. Yet, these studies refer to generally humid regions and cannot be extrapolated to more arid
533 climates. A related conclusion is proposed by Seneviratne et al. (2006) who found the highest soil moisture
534 memory for intermediate soil wetness. ~~There~~ These results do not contrast with our findings, which refer to
535 a wide range of climatic conditions.

536 We also confirm the role of lakes in determining higher catchment storage and therefore positive
537 correlations for the LFS, which has been reported for annual persistence in a few sites (Zhang et al., 2012).

538 The effect of snow cover for lag-1 LFS correlation is also revealed by the Austrian catchments. The
539 mountainous rivers, directly affected by the process of snow accumulation, exhibit winter LFS and higher
540 correlation than the rivers in the lowlands, which are more prone to drying out due to evapotranspiration in
541 the hotter summer months. The inspection of elevation data confirmed the role of high altitudes in

542 increasing LFS correlation, which is likely related to storage effects due to snow accumulation and gradual
543 melting. In this respect, Kuentz et al. (2017) found that topography exerts dominant controls over the flow
544 regime in the larger European region, controlling the flashiness of flow, and being a particularly important
545 driver for other low flow signatures too. In fact, topography may affect the flow regime directly, through
546 flow routing, but also indirectly, because of orographic effects in precipitation and hydroclimatic processes
547 affected by elevation (e.g. snowmelt and evapotranspiration).

548 Regarding atmospheric forcing, we find LFS correlation to be negatively correlated to mean areal
549 temperature and annual precipitation. The former result may be explained considering that increased
550 evapotranspiration (higher temperature) is expected to dry out LFS flows while snow coverage (lower
551 temperature) was found to be associated ~~to~~with higher LFS correlation. An apparently different conclusion
552 was drawn by Szolgayova et al. (2014a) and Gudmundsson et al. (2011), who reported increasing
553 persistence with increasing mean temperature postulating that snow-dominated flow regimes smooth out
554 interannual fluctuations. Yet, it should be noted that they refer to interannual variability while we refer here
555 to seasonal correlation and therefore to shorter time scales, which imply a different dynamic of snow
556 accumulation and snowmelt; latitude may also play a relevant role in this, since in southern Europe the
557 complete ablation of snow can occur more than once during the cold season, and sublimation may account
558 for 20–30-% of the annual snowfall (Herrero and Polo, 2016), decreasing the amount of snowmelt and
559 impacting LFS flows in the summer season.

560 Snowmelt mechanisms are found to increase predictive skill during low-flow periods in some other
561 studies (Bierkens and van Beek, 2009; Mahanama et al., 2011; Dijk et al., 2013). However, in the glacier-
562 dominated regime of western Alpine and central Austrian catchments this is not expected to be a relevant
563 driver of higher correlation, since low flow is occurring in the winter months. Yet the mountainous, glacier-
564 dominated rivers still show increased LFS correlation compared to rivers in the lowlands, which agrees
565 well with other studies that have found less uncertainty in the rainfall-runoff modelling in this regime

owing to the greater seasonality of the runoff process and the decreased impact of rainfall compared to the rainfall-dominated regime of the lowlands (e.g Parajka et al., 2016).

Although the considerable uncertainty of areal precipitation estimates should be acknowledged, the contribution of annual precipitation interestingly complements the negative effect of increasing specific runoff –which is highly correlated to P estimates– on the correlation magnitude for both LFS and HFS. This outcome confirms that catchments receiving significant amount of rainfall do show less correlation than drier regimes.

~~We conclude that our results are essentially in agreement with the relevant literature and point out the possibility to exploit river memory within a data assimilation context to reduce uncertainty in the prediction of future high and low flows. The opportunity of exploiting correlation is not affected by the presence of regulation, provided the management of river flow does not change in time. Therefore, river memory is an interesting option to inspect opportunities for improving the prediction of water-related natural hazards.~~

9. Conclusions and outlook

This research investigates the presence of persistence in river flow at the seasonal scale, the associated physical drivers and the prospect for employing the related information to improve probabilistic prediction of high and low flows. The main findings are summarized below:

- Rivers in Europe show persistent features at the seasonal timescale, manifested as correlation between high- and low-flow signatures, i.e. peak flows in HFS and average flows in LFS respectively, and average flows in the previous month. LFS correlation is found consistently higher than HFS correlation.
- Seasonal correlation shows increased spatial variability together with spatial clustering.
- Storage mechanisms, groundwater-dominated basins and slower catchment response time, as reflected by large basin areas, high baseflow index and the presence of lakes, amplify correlation. On the contrary, correlation is lower in quickly responding karstic basins, and increased wetness conditions, as revealed by high specific runoff.

Formatted: Heading 1

Formatted: Bulleted + Level: 1 + Aligned at: 0" + Indent at: 0.25"

• Low mean areal temperature is associated with higher LFS correlation owing to the weaker drying-out evapotranspiration force and the mechanism of snow accumulation in higher altitudes. Higher mean areal precipitation is associated with lower LFS predictability, possibly due to the presence of saturated conditions and increased short-term variability in wetter climates.

• The drivers of LFS predictability are easier to identify and allow for the opportunity to construct regression models for possible application to ungauged basins (see Section 6).

• HFS and LFS correlation may directly serve for the probabilistic prediction of ‘extremes’, i.e. high and low flows, as increased correlation can be exploited in various stochastic models. -Such an application was performed in Section 7 in a data assimilation setting for a river of marked technical relevance.

Regarding the latter, once a significant correlation is identified, it may be exploited in other model variants as well, e.g. adding more dependent variables of lagged flow and/or coupling with other relevant explanatory variables, such as teleconnections or antecedent rainfall, in multivariate prediction schemes.

Indeed, the presence of river memory at the seasonal scale represents a possible opportunity to improve the prediction of water-related natural hazards by reducing uncertainty of associated estimates and allowing significant lag time for decision-making and hazard prevention. Besides the high relevance for extremes, this type of seasonal predictability could also be of interest to water resources management by, for instance, exploring the memory properties of a minor HFS.

The inspection of the physical basis, apart from advancing our understanding of the catchment dynamics, is highly important as it may also guide the search for other dependent variables and build confidence in the formation of process-based stochastic models (Montanari and Koutsoyiannis, 2012). A large sample of indices was herein inspected, yet data are majorly needed to allow for more certain and generalized conclusions worldwide. An important note is the presence of regulation, the effect of which, due to lack of objective data, is not completely understood. However, the opportunity of exploiting correlation is not affected by the presence of regulation, provided that the management of river flow does not change in time.

We conclude that our results are essentially in agreement with the relevant literature and point out the possibility to exploit river memory within a data assimilation context to reduce uncertainty in the prediction of future high and low flows. The opportunity of exploiting correlation is not affected by the presence of regulation, provided the management of river flow does not change in time. Therefore, river memory provides interesting information – an interesting option – direction that holds both theoretical and operational potential to inspect opportunities for to improve the understanding and prediction of extremes water-related natural hazards, support decision-making and increase the level of preparedness for water-related natural hazards.

Formatted: English (United States)

Data and Code availability

The data and code used in this study may be made available to the readers upon request to the corresponding author.

Competing interests

The authors declare that they have no conflict of interest.

Acknowledgements

The present work was (partially) developed within the framework of the Panta Rhei Research Initiative of the International Association of Hydrological Sciences (IAHS). Part of the results were elaborated in the Switch-On Virtual Water Science Laboratory that was developed in the context of the SWITCH-ON (Sharing Water-related Information to Tackle Changes in the Hydrosphere – for Operational Needs) project, funded by the European Union Seventh Framework Programme (FP7/2007-2013) under grant agreement no. 603587. N. Bezak gratefully acknowledges funding by the Slovenian Research Agency (grants J2-7322 and P2-0180). M. Bermúdez gratefully acknowledges financial support from the Spanish Regional Government of Galicia, Postdoctoral Grant Program 2014.

References

- Aguilar, C., Montanari, A., Polo, M.-J., 2017. Real-time updating of the flood frequency distribution through data assimilation. *Hydrol. Earth Syst. Sci.* 21, 3687–3700. <https://doi.org/10.5194/hess-21-3687-2017>
- Barredo, J.I., 2007. Major flood disasters in Europe: 1950–2005. *Natural Hazards* 42, 125–148. <https://doi.org/10.1007/s11069-006-9065-2>
- Bierkens, M.F.P., van Beek, L.P.H., 2009. Seasonal Predictability of European Discharge: NAO and Hydrological Response Time. *Journal of Hydrometeorology* 10, 953–968. <https://doi.org/10.1175/2009JHM1034.1>
- Cervi, F., Blöschl, G., Corsini, A., Borgatti, L., Montanari, A., 2017. Perennial springs provide information to predict low flows in mountain basins. *Hydrological Sciences Journal* 62, 2469–2481. <https://doi.org/10.1080/02626667.2017.1393541>
- Chiew, F.H.S., Zhou, S.L., McMahon, T.A., 2003. Use of seasonal streamflow forecasts in water resources management. *Journal of Hydrology* 270, 135–144. [https://doi.org/10.1016/S0022-1694\(02\)00292-5](https://doi.org/10.1016/S0022-1694(02)00292-5)
- Conover, W.J., 1971. *Practical Nonparametric Statistics*. New York: John Wiley and Sons. Inc.
- Cunderlik, J.M., Ouarda, T.B., Bobée, B., 2004. Determination of flood seasonality from hydrological records/Détermination de la saisonnalité des crues à partir de séries hydrologiques. *Hydrological Sciences Journal* 49. <https://doi.org/10.1623/hysj.49.3.511.54351>
- De Martonne, E.M., 1926. L'indice d'aridité. *Bulletin de l'Association de géographes français* 3, 3–5. <https://doi.org/10.3406/bagf.1926.6321>
- Dijk, A.I., Peña-Arancibia, J.L., Wood, E.F., Sheffield, J., Beck, H.E., 2013. Global analysis of seasonal streamflow predictability using an ensemble prediction system and observations from 6192 small catchments worldwide. *Water Resources Research* 49, 2729–2746. <https://doi.org/10.1002/wrcr.20251>
- Dimitriadis, P., Koutsoyiannis, D., Tzouka, K., 2016. Predictability in dice motion: how does it differ from hydro-meteorological processes? *Hydrological Sciences Journal* 61, 1611–1622. <https://doi.org/10.1080/02626667.2015.1034128>
- Gabriel, K.R., 1971. The biplot graphic display of matrices with application to principal component analysis. *Biometrika* 58, 453–467. <https://doi.org/10.1093/biomet/58.3.453>
- Gower, J.C., Hand, D.J., 1995. *Biplots*. CRC Press.
- Gudmundsson, L., Tallaksen, L.M., Stahl, K., Fleig, A.K., 2011. Low-frequency variability of European runoff. *Hydrology and Earth System Sciences* 15, 2853–2869. <https://doi.org/10.5194/hess-15-2853-2011>
- Gustard, A., Demuth, S., others, 2009. *Manual on low-flow estimation and prediction*. Opera.
- Harman, C.J., Troch, P.A., Sivapalan, M., 2011. Functional model of water balance variability at the catchment scale: 2. Elasticity of fast and slow runoff components to precipitation change in the continental United States. *Water Resources Research* 47. <https://doi.org/10.1029/2010WR009656>
- Herrero, J., Polo, M.J. 2016. Evaporesublimation from the snow in the Mediterranean mountains of Sierra Nevada (Spain). *The Cryosphere*, 10, 2981–2998, <https://doi.org/10.5194/tc-10-2981-2016>
- Hirpa, F.A., Gebremichael, M., Over, T.M., 2010. River flow fluctuation analysis: Effect of watershed area. *Water Resources Research* 46. <https://doi.org/10.1029/2009WR009000>
- Hurst, H.E., 1951. Long-term storage capacity of reservoirs. *Trans. Amer. Soc. Civil Eng.* 116, 770–808.
- Jolliffe, I., 2002. *Principal component analysis*. Wiley Online Library. <https://doi.org/10.1002/9781118445112.stat06472>
- Kelly, K.S., Krzysztofowicz, R., 1997. A bivariate meta-Gaussian density for use in hydrology. *Stochastic Hydrology and hydraulics* 11, 17–31. <https://doi.org/10.1007/BF02428423>

Formatted: Bibliography

Formatted: English (United States)

- Kottek, M., Grieser, J., Beck, C., Rudolf, B., Rubel, F., 2006. World Map of the Köppen-Geiger climate classification updated. *Meteorologische Zeitschrift* 259–263. <https://doi.org/10.1127/0941-2948/2006/0130>
- Koutsoyiannis, D., 2011. Hurst-Kolmogorov Dynamics and Uncertainty. *JAWRA Journal of the American Water Resources Association* 47, 481–495. <https://doi.org/10.1111/j.1752-1688.2011.00543.x>
- Koutsoyiannis, D., Yao, H., Georgakakos, A., 2008. Medium-range flow prediction for the Nile: a comparison of stochastic and deterministic methods/Prévision du débit du Nil à moyen terme: une comparaison de méthodes stochastiques et déterministes. *Hydrological Sciences Journal* 53, 142–164. <https://doi.org/10.1623/hysj.53.1.142>
- Kuentz, A., Arheimer, B., Hundecha, Y. and Wagener, T., 2017. Understanding hydrologic variability across Europe through catchment classification. *Hydrology and Earth System Sciences*, 21(6), p.2863–2879, <https://doi.org/10.5194/hess-21-2863-2017>.
- Lee, D., Ward, P., Block, P., 2015. Defining high-flow seasons using temporal streamflow patterns from a global model. *Hydrology and Earth System Sciences* 19, 4689–4705. <https://doi.org/10.5194/hess-19-4689-2015>
- Mahanama, S., Livneh, B., Koster, R., Lettenmaier, D., Reichle, R., 2011. Soil Moisture, Snow, and Seasonal Streamflow Forecasts in the United States. *J. Hydrometeor.* 13, 189–203. <https://doi.org/10.1175/JHM-D-11-046.1>
- Markonis, Y., Moustakis, Y., Nasika, C., Sychova, P., Dimitriadis, P., Hanel, M., Máca, P., Papalexiou, S.M., 2018. Global estimation of long-term persistence in annual river runoff. *Advances in Water Resources* 113, 1–12. <https://doi.org/10.1016/j.advwatres.2018.01.003>
- Montanari, A., 2012. Hydrology of the Po River: looking for changing patterns in river discharge. *Hydrology and Earth System Sciences* 16, 3739–3747. <https://doi.org/10.5194/hess-16-3739-2012>
- Montanari, A., Brath, A., 2004. A stochastic approach for assessing the uncertainty of rainfall-runoff simulations. *Water Resources Research* 40. <https://doi.org/10.1029/2003WR002540>
- Montanari, A., Koutsoyiannis, D., 2012. A blueprint for process-based modeling of uncertain hydrological systems. *Water Resources Research* 48, <https://doi.org/10.1029/2011WR011412>
- Mudelsee, M., 2007. Long memory of rivers from spatial aggregation. *Water Resources Research* 43. <https://doi.org/10.1029/2006WR005721>
- O'Connell, P.E., Koutsoyiannis, D., Lins, H.F., Markonis, Y., Montanari, A., Cohn, T., 2016. The scientific legacy of Harold Edwin Hurst (1880–1978). *Hydrological Sciences Journal* 61, 1571–1590. <https://doi.org/10.1080/02626667.2015.1125998>
- Parajka, J., Blaschke, A.P., Blöschl, G., Haslinger, K., Hepp, G., Laaha, G., Schöner, W., Trautvetter, H., Viglione, A., Zessner, M., 2016. Uncertainty contributions to low-flow projections in Austria. *Hydrol. Earth Syst. Sci.* 20, 2085–2101. <https://doi.org/10.5194/hess-20-2085-2016>
- Parajka, J., Kohnová, S., Bálint, G., Barbuc, M., Borga, M., Claps, P., Cheval, S., Dumitrescu, A., Gaume, E., Hlavčová, K., others, 2010. Seasonal characteristics of flood regimes across the Alpine–Carpathian range. *Journal of hydrology* 394, 78–89. <https://doi.org/10.1016/j.jhydrol.2010.05.015>
- Parajka, J., Kohnová, S., Merz, R., Szolgay, J., Hlavčová, K., Blöschl, G., 2009. Comparative analysis of the seasonality of hydrological characteristics in Slovakia and Austria/Analyse comparative de la saisonnalité de caractéristiques hydrologiques en Slovaquie et en Autriche. *Hydrological Sciences Journal* 54, 456–473. <https://doi.org/10.1623/hysj.54.3.456>
- Piechota, T.C., Chiew, F.H., Dracup, J.A. and McMahon, T.A., 2001. Development of exceedance probability streamflow forecast. *Journal of Hydrologic Engineering*, 6(1), pp.20–28. [https://doi.org/10.1061/\(ASCE\)1084-0699\(2001\)6:1\(20\)](https://doi.org/10.1061/(ASCE)1084-0699(2001)6:1(20))
- Prudhomme, C., Hannaford, J., Harrigan, S., Boorman, D., Knight, J., Bell, V., Jackson, C., Svensson, C., Parry, S., Bachiller-Jareno, N., 2017. Hydrological Outlook UK: an operational streamflow and

Formatted: Font: (Default) Times New Roman, 12 pt

Formatted: Bibliography

Formatted: Font color: Text 1, English (United Kingdom)

Formatted: Font: (Default) Times New Roman, 12 pt

Formatted: Font: (Default) Times New Roman, 12 pt

groundwater level forecasting system at monthly to seasonal time scales. *Hydrological Sciences Journal* 62, 2753–2768. <https://doi.org/10.1080/02626667.2017.1395032>

Formatted: Font: (Default) Times New Roman, 12 pt

- Ravbar, N., 2013. Variability of groundwater flow and transport processes in karst under different hydrologic conditions/Spremenljivost Pretakanja Voda in Prenosa Snovi V Krasu ob Razlicnih Hidroloskih Pogojih. *Acta Carsologica* 42, 327. <http://dx.doi.org/10.3986/ac.v42i2.644>
- Seneviratne, S.I., Koster, R.D., Guo, Z., Dirmeyer, P.A., Kowalczyk, E., Lawrence, D., Liu, P., Mocko, D., Lu, C.-H., Oleson, K.W., others, 2006. Soil moisture memory in AGCM simulations: analysis of global land–atmosphere coupling experiment (GLACE) data. *Journal of Hydrometeorology* 7, 1090–1112. <https://doi.org/10.1175/JHM533.1>
- Spearman, C., 1904. The Proof and Measurement of Association between Two Things. *The American Journal of Psychology* 15, 72–101. <https://doi.org/10.2307/1412159>
- Svensson, C., 2016. Seasonal river flow forecasts for the United Kingdom using persistence and historical analogues. *Hydrological Sciences Journal* 61, 19–35. <https://doi.org/10.1080/02626667.2014.992788>
- Szolgayova, E., Laaha, G., Blöschl, G., Bucher, C., 2014. Factors influencing long range dependence in streamflow of European rivers. *Hydrological Processes* 28, 1573–1586. <https://doi.org/10.1002/hyp.9694>
- Wang, Q.J., Robertson, D.E., Chiew, F.H.S., 2009. A Bayesian joint probability modeling approach for seasonal forecasting of streamflows at multiple sites. *Water Resources Research* 45. <https://doi.org/10.1029/2008WR007355>
- Willsher, K., 2005. France brings in water rationing after worst drought for 30 years. *The Guardian*. <https://www.theguardian.com/environment/2005/jul/11/weather.france>
- Yossef, N.C., Winsemius, H., Weerts, A., Beek, R., Bierkens, M.F., 2013. Skill of a global seasonal streamflow forecasting system, relative roles of initial conditions and meteorological forcing. *Water Resources Research* 49, 4687–4699. <http://dx.doi.org/10.1002/wrcr.20350>
- Zhang, Q., Zhou, Y., Singh, V.P., Chen, X., 2012. The influence of dam and lakes on the Yangtze River streamflow: long-range correlation and complexity analyses. *Hydrological Processes* 26, 436–444. <http://dx.doi.org/10.1002/hyp.8148>

Tables

Table 1 Summary statistics of the river descriptors. Summary statistics for PL, PG and PF variables are computed only for the subset of catchments with positive values (the total number of catchments is also reported in brackets). PK is used as a categorical variable (PK is either higher or lower than 50-% of catchment area), therefore sample statistics are not computed in this case, but the number of stations with $PK \geq 50\%$ is reported as ‘positive’ presence of karst.

Descriptor (Units)	A (km ²)	BI (–)	SR (m ³ s ^{–1} km ^{–2})	PL (%)	PG (%)	PF (%)	PK (–)	P (mm year ^{–1})	T (°C)	IDM (–)
Min	4.7	0.29	0.004	0.5	0.1	0.3	–	444	–1.8	29.41
Max	70091	0.99	0.088	19.5	56.5	100	–	1500	13.7	153.40

Standard deviation	5904.3	0.14	0.018	4.04	15.54	32.56	—	288.22	3.59	24.53
Sample size	224	224	224	69 [69]	39 [108]	18 [108]	21 [31]	224	224	224

Table 2 Differences in the mean values between the descriptors of the 20-highest correlation river group for HFS and LFS vs the remaining rivers (204). N_L , N_G , N_F and N_K columns contain the absolute number of rivers in the higher correlation group with the specific descriptor (presence of lake, glacier, flysch and karst) with * denoting significance at 5-% significance level (two-sided test) and brackets containing the mean value from the 1000 resampled 20-catchment subsets.

Descriptor (Units)	A (km ²)	BI (—)	SR (m ³ s ⁻¹ km ⁻²)	N_L (—)	N_G (—)	N_F (—)	N_K (—)	P (mm year ⁻¹)	T (°C)	IDM (—)
HFS lag1	+38.7-%	+9.6-%	−36.5-%	5 [6]	5 [3]	1 [2]	1 [2]	−6.7-%	+11.7-%	−11.3-%
LFS lag1	+358-%	+20.2-%	−47.3-%	17* [6]	3 [3]	0 [2]	0 [2]	−37.9-%	−80-%	−17.3-%
LFS lag2	+139.7-%	+18.9-%	−40.8-%	12* [6]	7* [3]	0 [2]	0 [2]	−26.5-%	−64.2-%	−8.8-%

Table 3 Loadings of the three Principal Components for $\ln A$, SR, BI and T . The explained variance of each PC is denoted in parenthesis.

790

791

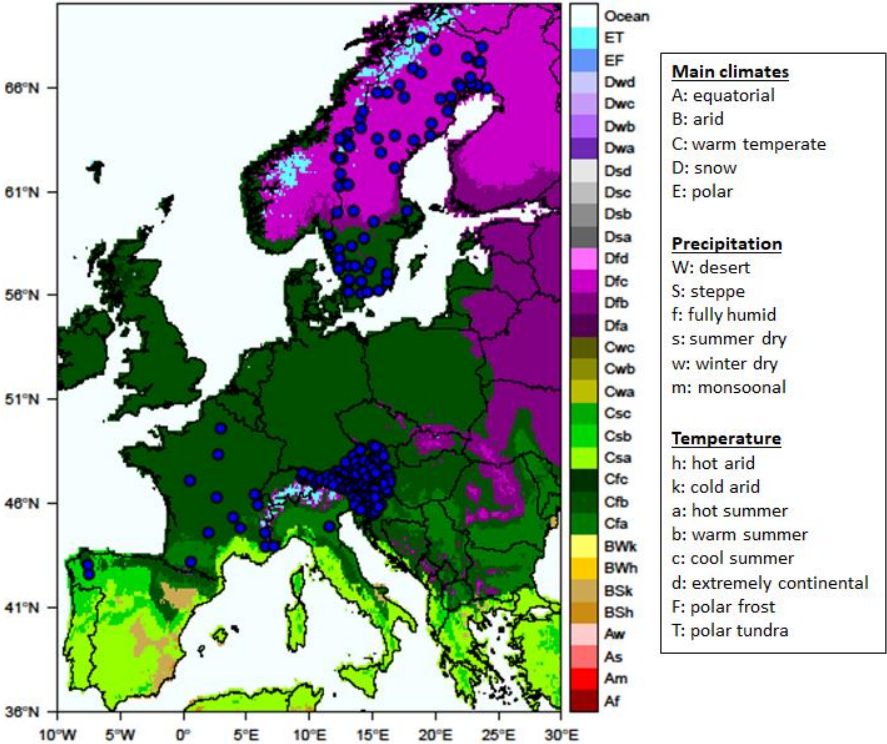
792

793

Predictor variables	PC1 (42.5-%)	PC2 (28.2-%)	PC3 (17-%)	PC4 (12.2-%)
ln A	−0.486	−0.427	0.748	0.145
SR	0.48	0.483	0.652	−0.332
BI	−0.619	0.262	−0.11	−0.731
T	0.385	−0.718	−0.04	−0.577

Table 4 Summary of Linear Regression results for the LFS model. *** indicate a 0.1-% significance level.

Predictor variables	Estimate	Standard Error	t value	Pr(> t)	Adjusted R ²	F-statistic
intercept	0.659407	0.008557	77.065	$< 2 \times 10^{-16}$ ***	0.5834	104.2
PC1	−0.110632	0.006577	−16.820	$< 2 \times 10^{-16}$ ***		p-value:
PC2	0.031761	0.008070	3.936	0.000111***		$< 2.2 \times 10^{-16}$
PC3	−0.038999	0.010388	−3.754	0.000223***		



795

796 **Figure 1.** Updated Köppen-Geiger climatic map for period 1951–2000 (Kottek et al., 2006) showing the location of
797 the 224 river gauge stations.

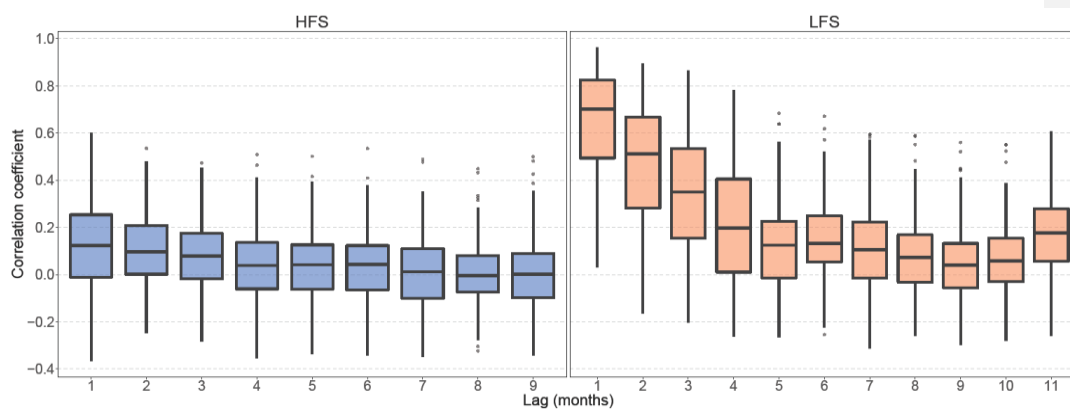


Figure 2. Boxplots of seasonal correlation coefficient against lag time for HFS (left panel) and LFS (right panel) analysis [for the 224 rivers](#). The lower and upper ends of the box represent the 1st and 3rd quartiles, respectively, and the whiskers extend to the most extreme value within 1.5 IQR (interquartile range) from the box ends; outliers are plotted as filled circles.

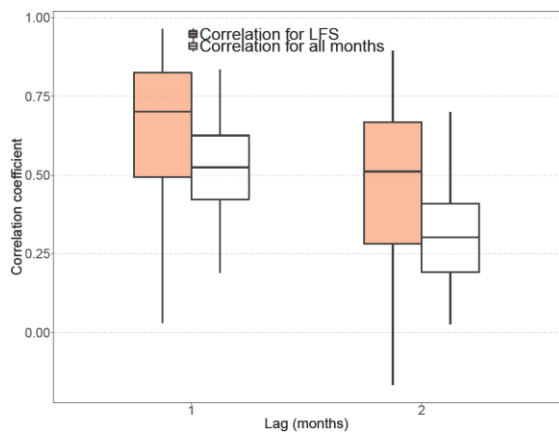
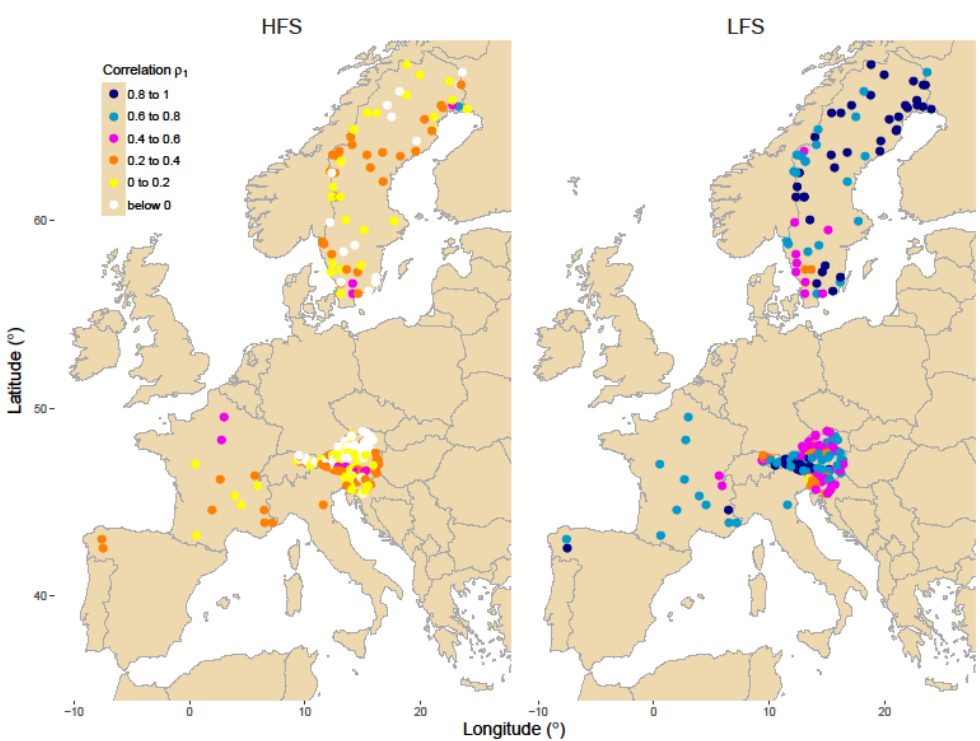


Figure 3. Boxplots of lag-1 and lag-2 correlation coefficients for LFS analysis (orange) and the whole monthly series (white) [for the 224 rivers](#). The lower and upper ends of the box represent the 1st and 3rd quartiles, respectively, and the whiskers extend to the most extreme value within 1.5 IQR (interquartile range) from the box ends.

\$08

\$09



Field Code Changed

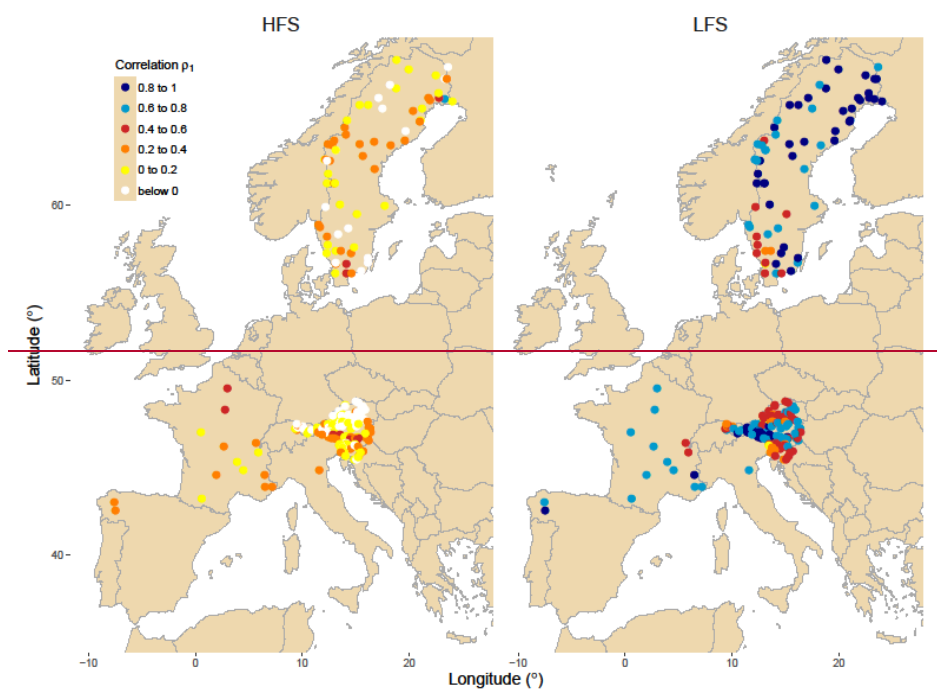


Figure 4. Spatial distribution of the lag-1 correlation coefficients for HFS (left) and LFS (right) analysis. Legend shows the color assigned to each class of correlation for the data.

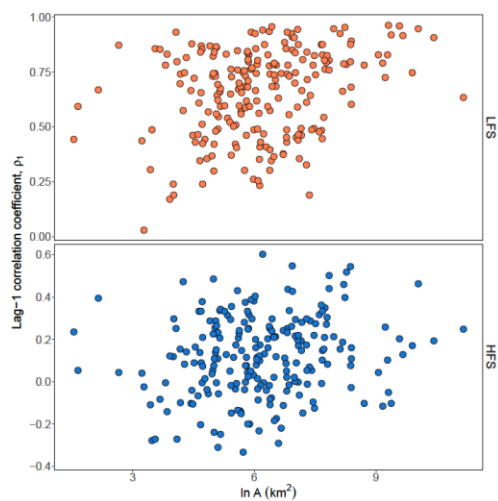


Figure 5. Scatterplots of lag-1 HFS (bottom panel) and LFS (top) streamflow correlation versus the natural logarithm of basin area $\ln A$.

Formatted: Font: Italic

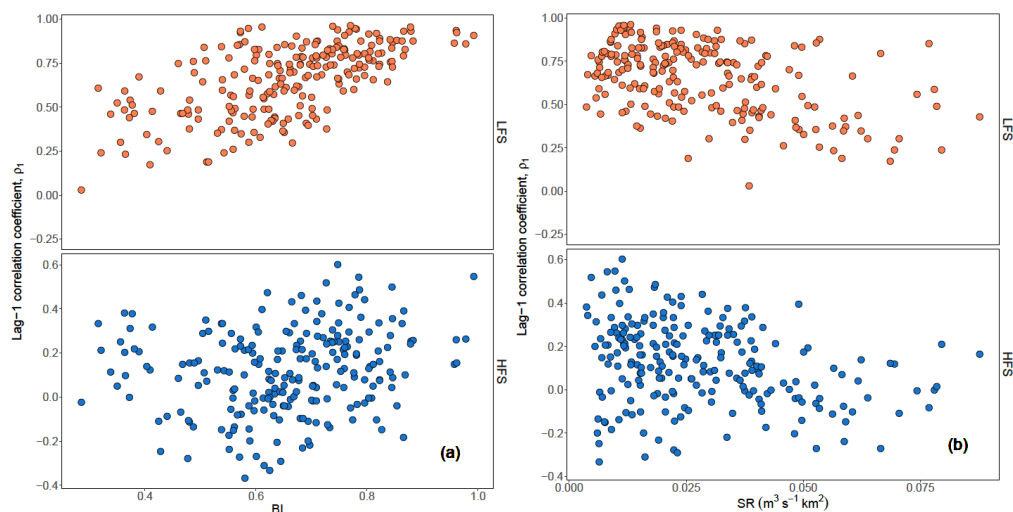


Figure 6. Scatterplots of lag-1 HFS (bottom panels) and LFS streamflow correlation (top panels) versus baseflow index BI (a) and specific runoff SR (b).

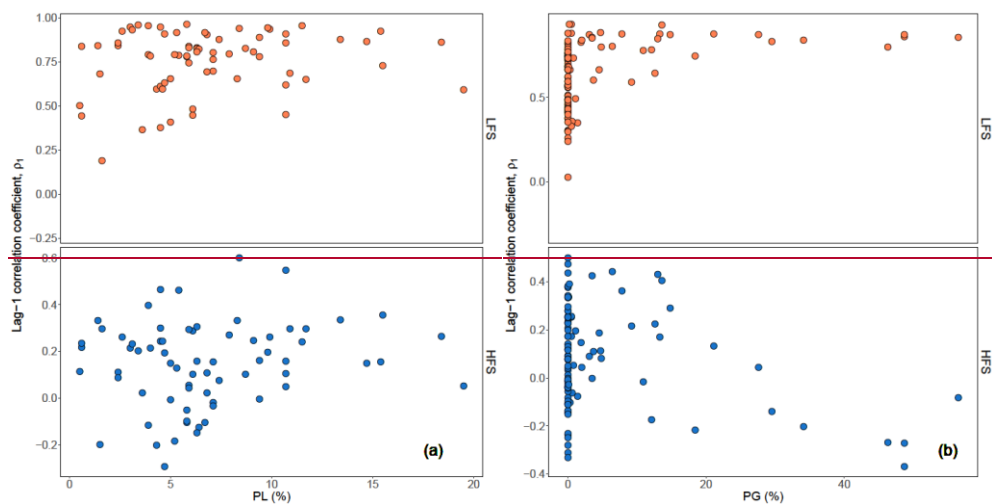
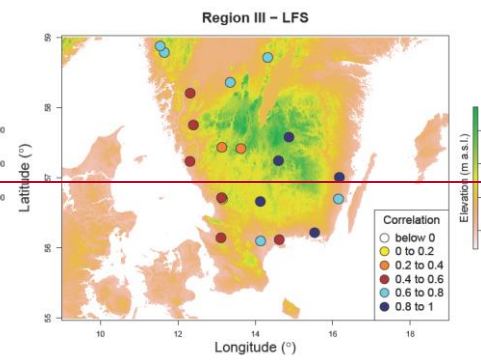
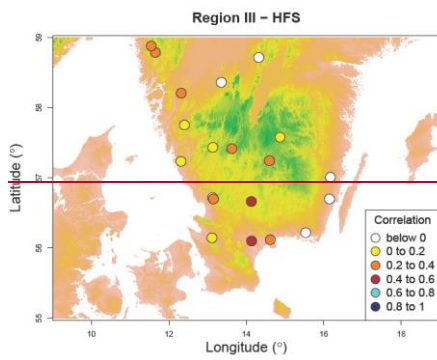
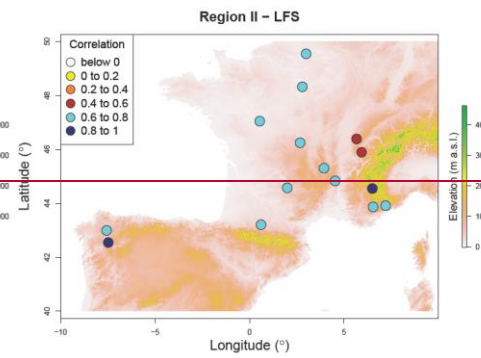
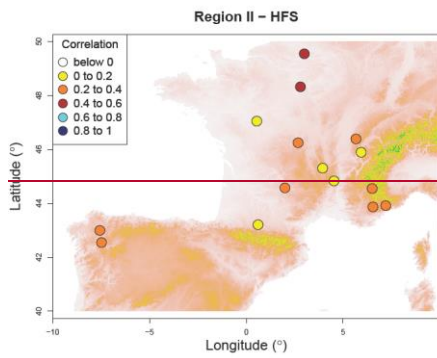
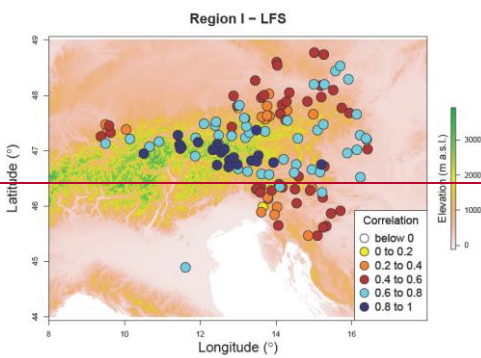
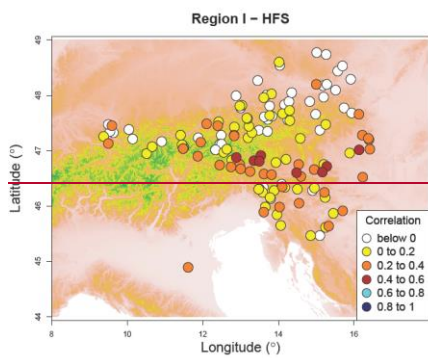
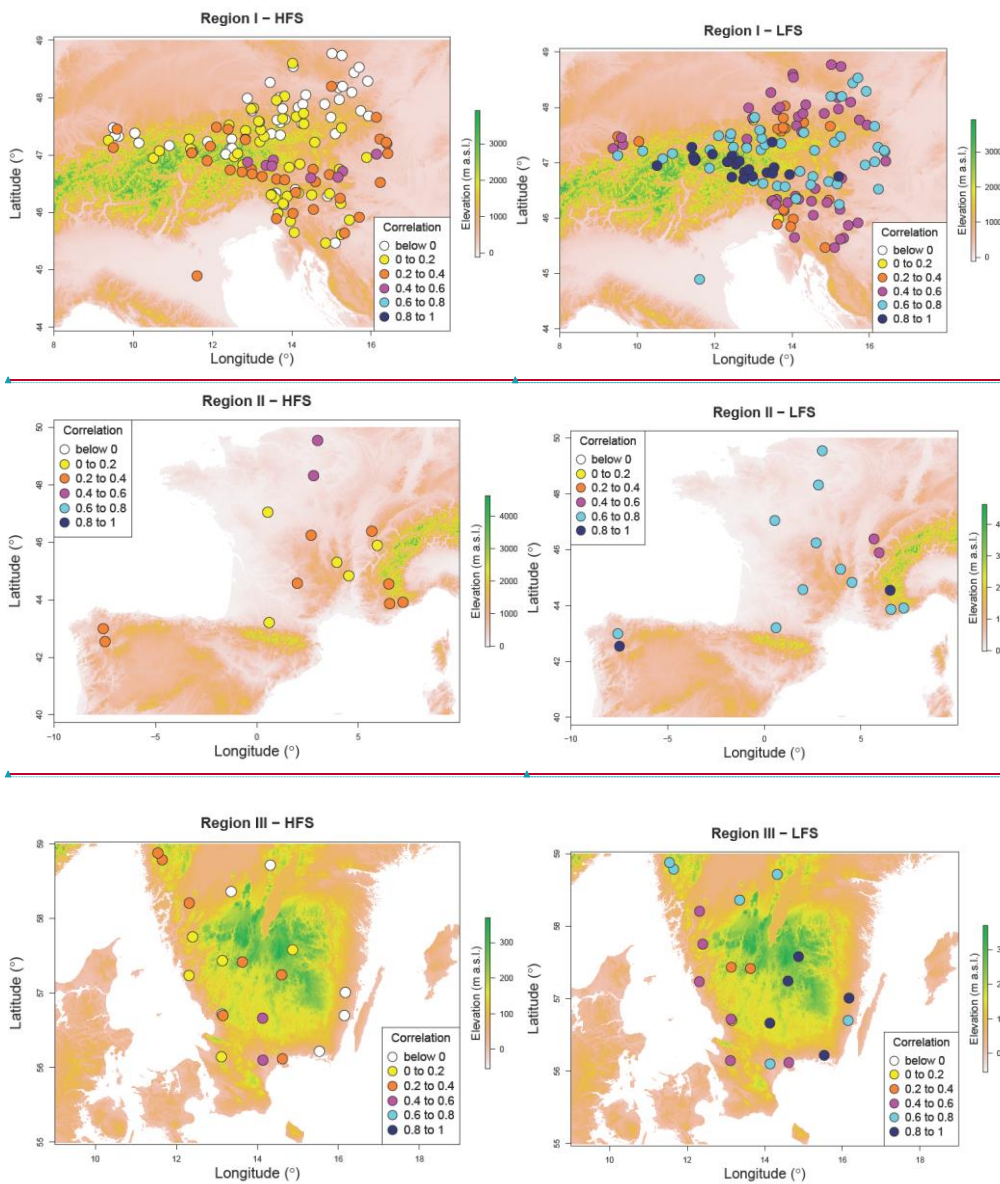


Figure 7. Scatterplots of lag-1 HFS (bottom) and LFS (top) streamflow correlations versus percentage of lakes PL of the Swedish catchments (a) and percentage of glaciers PG of the Austrian catchments (b).



Formatted: Normal



Field Code Changed

Field Code Changed

Field Code Changed

Field Code Changed

Field Code Changed

Field Code Changed

Figure 87. Relief maps from SRTM elevation data for the HFS and LFS lag-1 correlations of the rivers. Note that elevation scale is different for each region. Legend shows the colour assigned to each class of correlation for the data.

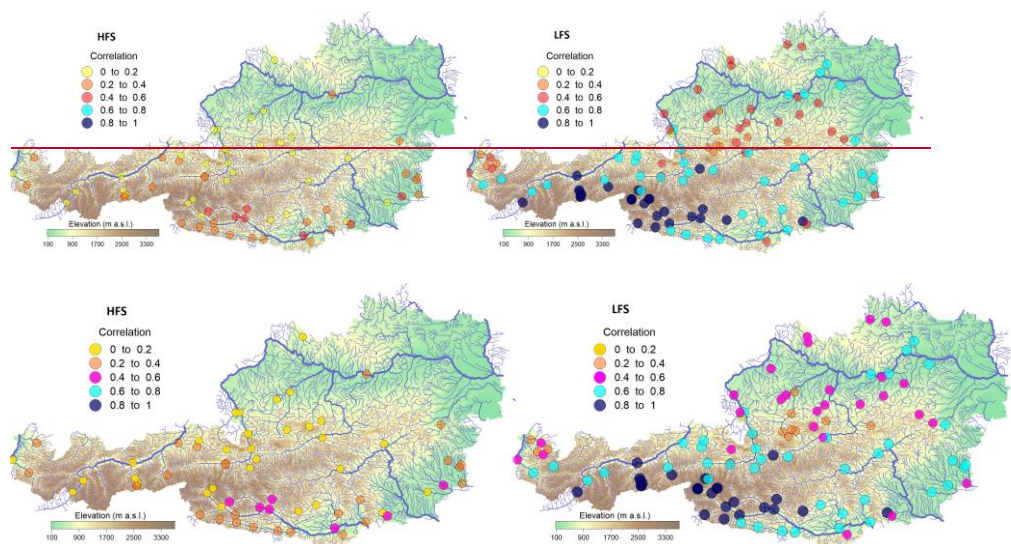


Figure 98. Digital elevation model of the Austrian river network depicting the spatial distribution of lag-1 positive correlation for HFS (left) and lag-1 positive correlation for LFS (right). Legend shows the colour assigned to each class of correlation for the data.

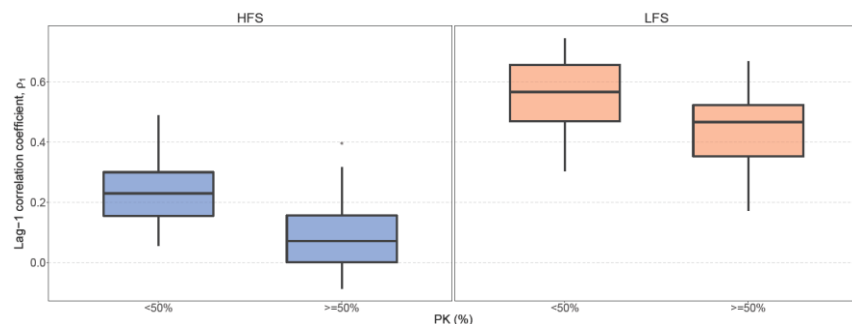


Figure 109. Boxplots of lag-1 correlation for Slovenian rivers with more than 50% presence of karstic formations PK and rivers with no or less presence for HFS analysis (left) and LFS analysis (right). The lower and upper ends of the box represent the 1st and 3rd quartiles, respectively, and the whiskers extend to the most extreme value within 1.5 IQR (interquartile range) from the box ends.

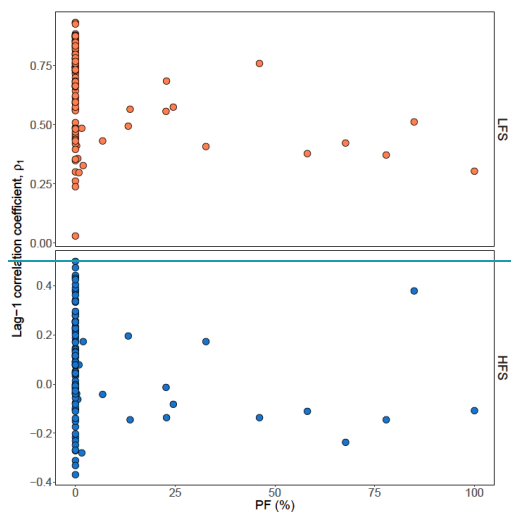


Figure 11. Scatterplots of lag-1 correlation vs percentage of flysch area coverage PF for HFS (bottom) and LFS (top) analysis for the Austrian catchments.

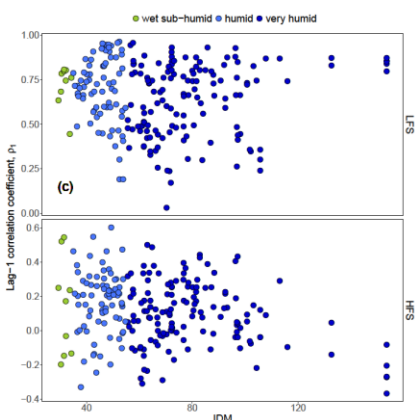
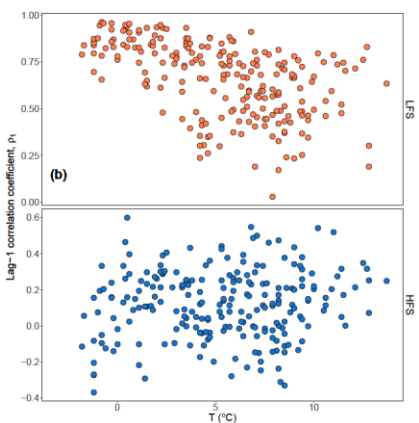
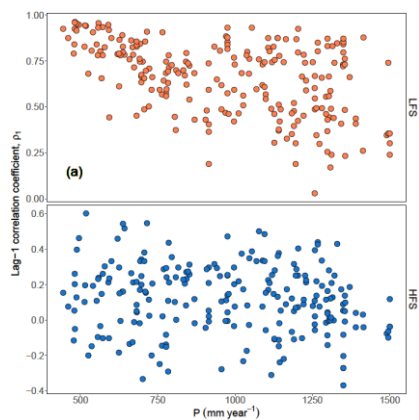


Figure 1210. Scatterplots of lag-1 HFS and LFS correlation versus annual precipitation P (a), mean annual temperature T (b), and Index De Martonne IDM (c).

Formatted: Font: 12 pt

Formatted: Font: 12 pt, Italic

Formatted: Font: 12 pt

Formatted: Font: 12 pt, Italic

Formatted: Font: 12 pt

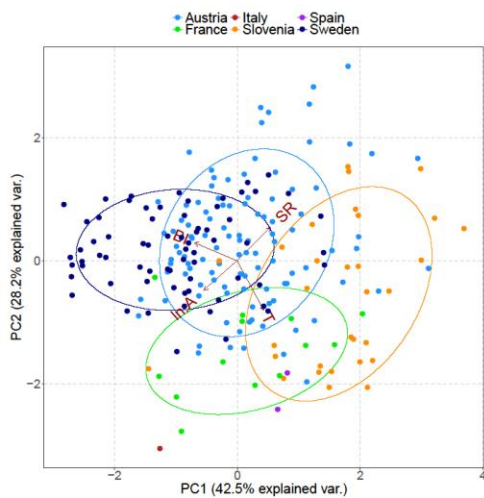


Figure 1411. Principal component distance biplot showing the principal component scores on the first two principal axes along with the vectors (brown arrows) representing the coefficients of the baseflow index BI, specific runoff SR, natural logarithm of basin area $\ln A$ and mean annual temperature T variables when projected on the principal axes. Scores for the rivers are plotted in different colors corresponding to each country of origin and 68% normal probability contour plots are plotted for the countries.

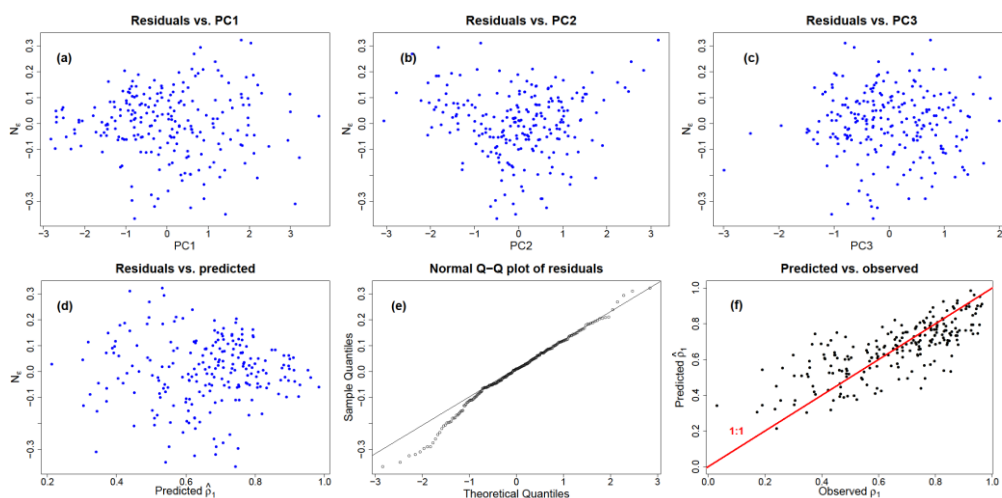
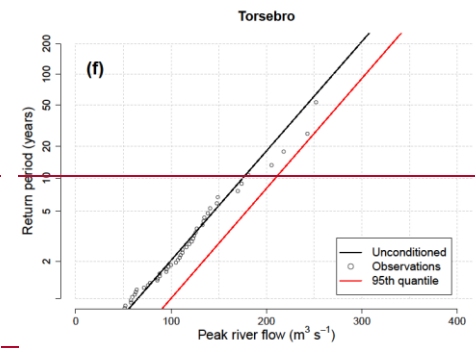
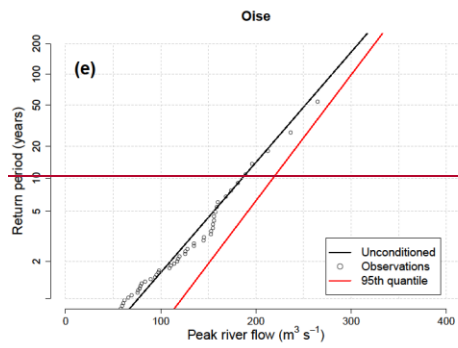
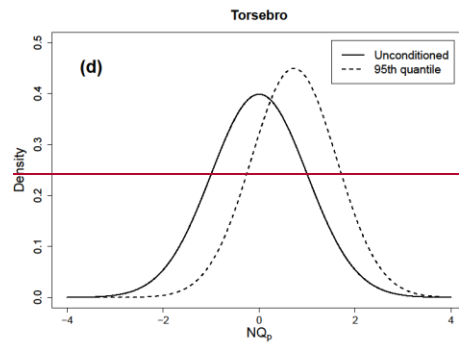
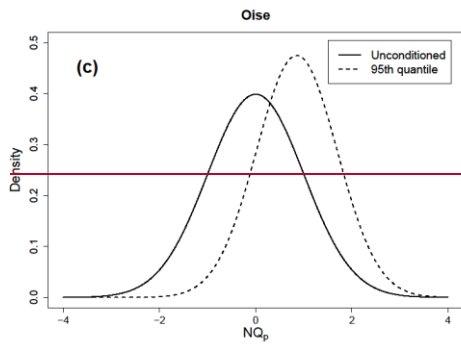
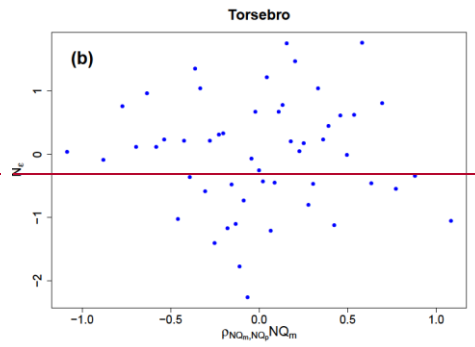
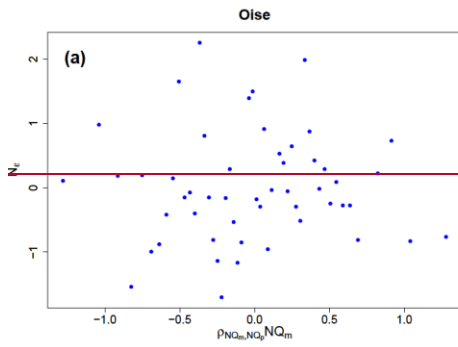
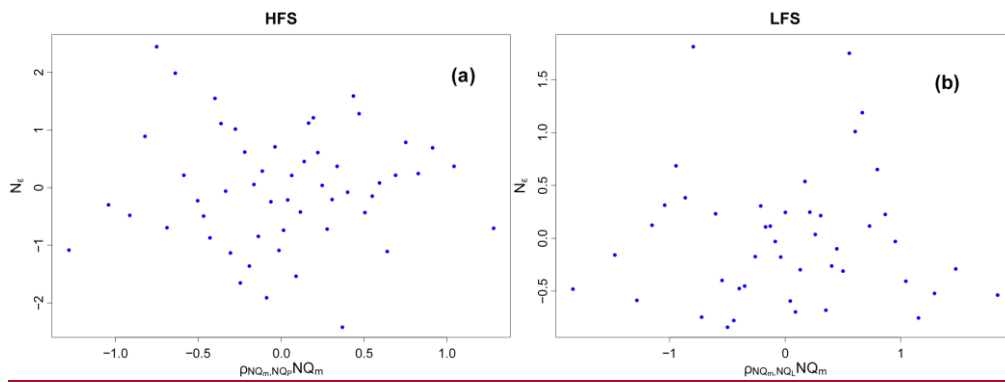


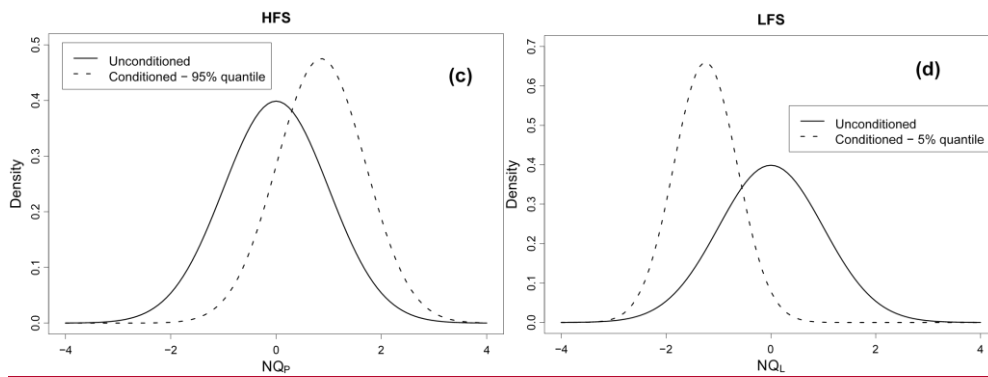
Figure 1412. Diagnostic plots of linear regression for the LFS model. Residuals versus the first (a), the second (b) and the third principal component (c) and the predicted values (d). Normal Q-Q plot of the residuals (e). Plot of the predicted values from linear regression vs the observed ones; red line is the diagonal line 1:1 (f).



Formatted: List Paragraph



Formatted: Normal



Field Code Changed

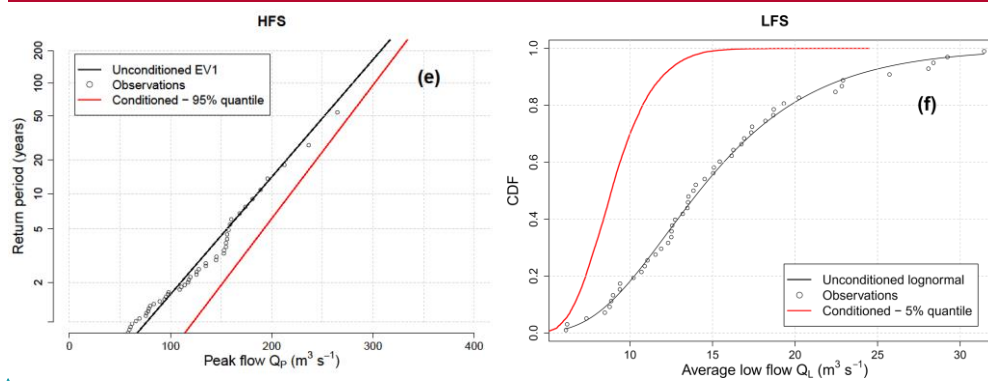


Figure 15.13. Conditioning the flood-frequency distributions for high and low flows for the Oise River and the Torsebro River. Plots of the residuals of the linear regression given by Eq. (2) for the Oise RHFS river (a) and the LFS Torsebro River (b) models. Probability distribution of the unconditioned normalized peak flows NQ_p/NQ_p (solid line) and the normalized peak flows NQ_p/NQ_p conditioned to the occurrence of the 95% quantile (dotted line) for the Oise River (c) and probability distribution of the unconditioned normalized low flows NQ_L (solid line) and the normalized low flows NQ_L conditioned to the occurrence of the 5% quantile (dotted line) for the LFS Torsebro River (d). Gumbel probability plots of the return period vs the unconditioned peak flows Q_p-Q_p (black line) and the peak flows Q_p-Q_p modelled by the EV1 distribution and conditioned to the occurrence of the 95-% quantile (red line) for the Oise River (e) and cumulative distribution function of the unconditioned low flows Q_L (black line) and the low flows Q_L modelled by the lognormal distribution and conditioned to the occurrence of the 5-% quantile (red line) for the LFS Torsebro River (f).